Bifurcation diagrams and heteroclinic networks of octagonal H-planforms

Grégory Faye[1] and Pascal Chossat[1,2]

[1]NeuroMathComp Laboratory, INRIA, Sophia Antipolis, CNRS, ENS Paris, France
[2]J-A Dieudonné Laboratory, CNRS and University of Nice Sophia-Antipolis, Parc Valrose, 06108 Nice Cedex 02, France

April 4, 2011

Abstract

This paper completes the classification of bifurcation diagrams for H-planforms in the Poincaré disc $\mathcal{D}$ whose fundamental domain is a regular octagon. An H-planform is a steady solution of a PDE or integro-differential equation in $\mathcal{D}$, which is invariant under the action of a lattice subgroup Γ of $U(1,1)$, the group of isometries of $\mathcal{D}$. In our case Γ generates a tiling of $\mathcal{D}$ with regular octagons. This problem was introduced in [15] as an example of spontaneous pattern formation in a model of image features detection by the visual cortex where the features are assumed to be represented in the space of structure tensors. Under "generic" assumptions the bifurcation problem reduces to an ODE which is invariant by an irreducible representation of the group of automorphisms $\mathcal{G}$ of the compact Riemann surface $\mathcal{D}/\Gamma$. The irreducible representations of $\mathcal{G}$ have dimension one, two, three and four. The bifurcation diagrams for the representations of dimension less than four have been obtained in [15] and correspond to already well known goup actions. In the present work we compute the bifurcation diagrams for the remaining three irreducible representations of dimension four, henceforth completing this classification. An interesting finding is that in one of these cases, there is generic bifurcation of a heteroclinic network connecting equilibria with two different orbit types.

Keywords: Equivariant bifurcation analysis; neural fields; Poincaré disc; heteroclinic network.

1 Introduction

Pattern formation through Turing mechanism is a well-known phenomenon [28]. For a system of reaction-diffusion equations defined in $\mathbb{R}^p$, with $p = 2$ or 3 say, it occurs when a neutrally stable linear mode is selected for a basic, homogeneous state, as a bifurcation parameter reaches a critical value. For the analysis of this phenomenon, the assumption that the system is invariant under the Euclidean transformations in the plane is essential. The problem is highly degenerate because any Fourier mode whose wave vector has critical length is a neutral stable mode. However in experiments as well as in numerical simulations it is often seen that the patterns which emerge above threshold, although they have a wave number equal or close to the critical one, are associated with a finite (and small) number of wave vectors which generate a *spatially periodic pattern* in the plane. This pattern is invariant under the action of a discrete translation subgroup Γ of $\mathbb{R}^p$. By looking at the class of states which respect this periodicity, or, what is the same, by looking at the system projected onto the torus $\mathbb{R}^p/\Gamma$, one removes the degeneracy: the critical wave vectors are in finite number, hence the critical eigenvalue has finite multiplicity and standard methods of equivariant bifurcation theory (see [12, 22]) can be applied to compute bifurcated solutions within this class of Γ-periodicity. Such solutions are called "planforms".

In a recent paper [15], a similar problem arose, but instead of being posed in the Euclidean plane, it was posed on the hyperbolic plane or, more conveniently, on the Poincaré disc. This problem originates from modeling the cortical perception of visual features, which we quickly describe now.

Neuronal representations of the external world are often based on the selectivity of the responses of individual neurons to external features. It has been well documented that neurons in the primary visual cortex respond preferentially to visual stimuli that have specific features such as orientation, spatial frequency, etc. Subgroups of inhibitory and excitatory neurons tuned to a particular feature of an external stimulus form what is called a *Hubel and Wiesel hypercolumn* of the visual area V1 in the cortex, roughly 1 mm^2 of cortical surface. Modeling the processing of image orientations has led Wilson and Cowan [41, 42] to derive a nonlinear integro-differential description of the evolution of the average action potential V in the hypercolumns. In an attempt to extend this model to other features (edge and corner detection, contrast...), it was proposed by [14] to assume that hypercolumns are sensitive to a nonlinear representation of the image first order derivatives called the structure tensor [6, 32]. Hence the average action potential is now a function of the structure tensors and time. Structure tensors are essentially 2×2 symmetric, definite positive matrices. They therefore live in a solide open cone in $\mathbb{R}^3$, which is a Riemannian manifold foliated by hyperbolic planes. By a suitable change of coordinates, the hyperbolic plane can be further identified with the Poincaré disc $\mathcal{D} = \{z \in \mathbb{C} \mid |z| < 1\}$. There is therefore an isomorphism between the space of structure tensors and the product space $\mathbb{R}_*^+ \times \mathcal{D}$, the distance on which being given by

$$d(\delta, z; \delta', z') = \sqrt{\log^2(\frac{\delta}{\delta'}) + \operatorname{arctanh} \frac{|z - z'|}{|1 - \bar{z}z'|}^2} \tag{1}$$

where the second term under the radical is the usual "hyperbolic" distance in $\mathcal{D}$.

The Wilson-Cowan equation on the space of structure tensors has the form

$$\partial_t V(\delta, z, t) = -V(\delta, z, t) + \int_{\mathbb{R}_*^+ \times \mathcal{D}} W(\delta, z, \delta', z') S(\mu V(\delta', z', t)) \mathrm{dm}(\delta', z') + I_{\text{ext}}(\delta, z, t) \tag{2}$$

The nonlinearity S is a smooth sigmoidal function ($S(x) \to \pm 1$ as $x \to \pm\infty$) with $S(0) = 0$. Note that $V = 0$ is always solution (trivial state) when $I_{\text{ext}} = 0$. The parameter μ describes the stiffness of the sigmoid. I_{ext} is an external input coming from different brain areas such as the thalamus and $W(\delta, z, \delta', z')$ expresses interactions between populations of neurons of types (δ, z) and (δ', z') in the hypercolumn. It is natural to assume that the connectivity function W does in fact only depend upon the distance between (δ, z) and (δ', z') : $W(\delta, z, \delta, z') = w(d(W(\delta, z; \delta, z'))$. Under this hypothesis, W is invariant by any isometric transformation in the space of structure tensors. If in addition $I_{ext} = 0$ (no input), equation (2) itself is invariant by any isometric transformation.

We shall from now on assume W of the above invariant form and $I_{ext} = 0$, and we look at possible bifurcations from trivial state as the stifness parameter μ is varied. We shall moreover forget about the part $\mathbb{R}_*^+$ with coordinate δ, because as was shown in [15], this part does not play a significant role in the subsequent analysis and it can be simply eliminated. From now on equation (2) is therefore posed on the 2D hyperbolic surface $\mathcal{D}$.

Spectral analysis in $\mathcal{D}$ requires the tools introduced by Helgason to perform Fourier analysis with respect to the coordinates in the Poincaré disc, namely the expansion of the solutions of the linearized system in elementary eigenfunctions of the Laplace-Beltrami operator [27]. These elementary eigenfunctions $e_{\rho,b}(z)$ depend on the "wave number" $\rho \in \mathbb{R}$ and point b on the boundary of the unit disc, and correspond to eigenvalues $1/4 + \rho^2$. Note that the eigenvalues are independant of the angle b. The function $e_{\rho,b}$ corresponds to a wavy pattern in $\mathcal{D}$ which is invariant along horocycles[1] with base point b and wavy along the geodesics with direction b. These functions are the hyperbolic counterparts of the elementary wavy eigenfunctions of the Laplacian in $\mathbb{R}^2$. As shown in [14], a critical value μ_c exists, but the same kind of rotational degeneracy occurs in this bifurcation problem as in Euclidean space: if ρ_c is the critical wave number, any $e_{\rho_c,b}$ is a neutrally stable eigenfunction, independently of the value of b. Moreover the spectrum is continuous. In order to apply equivariant bifurcation theory, we therefore need to look at a class of solutions which are *periodic* in $\mathcal{D}$, that is, solutions which are invariant under the action of a discrete subgroup Γ of $U(1,1)$ whose fundamental domain is a polygon. Such a subgroup is called a cocompact Fuchsian group and we can restrict further to look for such groups which contain no elliptic elements nor reflections[2]. Tilings of the Poincaré disc have very different properties from tilings

[1] A horocycle with base point b is a circle in $\mathcal{D}$, tangent at b to $\partial\mathcal{D}$.

[2] These subgroups of $SU(1,1)$ contain only hyperbolic elements and are the exact counterparts of discrete translation subgroups of $\mathbb{R}^p$. They are called "torsion-free" cocompact Fuchsian groups, see [29].

of the Euclidean plane. In particular tilings exist with polygons having an arbitrary number of sides, while in $\mathbb{R}^2$ only rectangular, square and hexagonal periodic tilings exist. Now the problem comes back to looking for bifurcated solutions of the equation defined on the quotient space $\mathcal{D}/\Gamma$, which is a compact Riemann surface and therefore on which the spectrum of the linearized operator is discrete and consists of eigenvalues with finite multiplicity.

This approach was presented in [15] and an example was studied, namely the case where the group Γ corresponds to a tiling of $\mathcal{D}$ with regular octagons. In this case Γ is generated by four hyperbolic transformations which are rotated from each other by angles $k\pi/4$ ($k = 1, 2, 3$), and $\mathcal{D}/\Gamma$ is a double torus (genus 2 surface). Moreover the group of automorphisms $\mathcal{G}$ of $\mathcal{D}/\Gamma$ is known and has 96 elements. Restricting to the class of Γ-periodic functions, our bifurcation problem is now reduced to an equation which is invariant under the action of $\mathcal{G}$. By standard center manifold reduction, this equation can be projected onto the critical eigenspace of the linearized operator. In our case the critical eigenvalue is 0 ("steady state" bifurcation) and its eigenspace is an absolutely irreducible representation space of the group $\mathcal{G}$.

In the same paper we have listed and described the 13 irreducible representations of $\mathcal{G}$ which we name $\chi_1, \cdots, \chi_{13}$: representations $\chi_1, \cdots, \chi_4$ have dimension one, χ_5, χ_6 have dimension two, $\chi_7, \cdots, \chi_{10}$ have dimension three and $\chi_{11}, \cdots, \chi_{13}$ have dimension four. Each of these cases leads to a different bifurcation diagram. We have listed all maximal isotropy subgroups and shown that their fixed point subspaces are one dimensional, hence we have found all branches of equilibria with maximal isotropy types by applying the Equivariant Branching Lemma [22]. Moreover we have shown that the bifurcation problems for the 2D cases is equivalent to problems with triangular symmetry, and in the 3D cases, to problems with octahedral symmetry. It follows that the bifurcation diagrams in these cases are known and show generically no other bounded dynamics than the trivial ones associated with the equilibria with maximal isotropy. There is no such identification in the 4D case. The aim of this paper is to fill this gap, by studying the bifurcation diagrams and local dynamics in the 4D irreducible representation spaces of $\mathcal{G}$. This will require a precise knowledge of these representations and of the Taylor expansion of vector fields which are equivariant by these representations (up to a sufficient order).

The structure of the paper is as follows:

- In section 2 we introduce the octagonal lattice and its symmetries, we recall the structure of the group $\mathcal{G}$ of automorphisms of $\mathcal{D}/\Gamma$ and its irreducible representations. We also recall the main result of [15] about the bifurcation of H-planforms in this case.
- In section 3, we study the case of the 4-dimensional irreducible representations χ_{12}, χ_{13} and show that the system is locally "gradient-like", implying that the only ω-limit sets are equilibria. The main results of this section are stated in theorems 2 and 3.
- In section 4, we focus on the analysis of the 4-dimensional irreducible representations χ_{11}. The computation of quintic equivariant vector fields is necessary to get a complete bifurcation diagram in the fixed point planes. We show that for some open range of the coefficients of quintic order terms, bifurcation with submaximal isotropy does occur. The main results are presented in theorems 4 and 5.
- In section 5, we both show the existence of a heteroclinic network and adress the question of its asymptotic stability. We illustrate this section with some numerical simulations.

2 Basic facts and results

In this section we recall some basic facts about the Poincaré disc and its isometries and we summarize results of [15] which will be useful in subsequent analysis.

2.1 The regular octagonal lattice and its symmetries

We recall that the direct (orientation preserving) isometries of the Poincaré disc $\mathcal{D}$ form the group $\mathrm{SU}(1,1)$ of 2×2 Hermitian matrices with determinant equal to 1. Given

$$\gamma = \begin{pmatrix} \alpha & \beta \\ \bar{\beta} & \bar{\alpha} \end{pmatrix} \text{ such that } |\alpha|^2 - |\beta|^2 = 1,$$

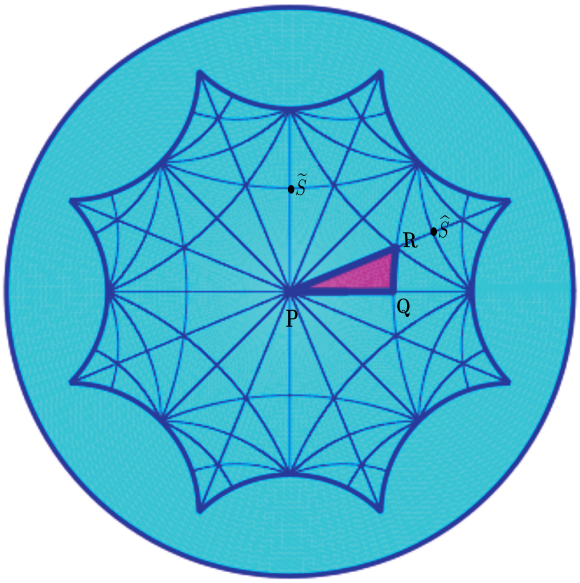

Figure 1: Tesselation of the hyperbolic octagon $\mathcal{O}$ with congruent triangles.

the corresponding isometry in $\mathcal{D}$ is defined by:

$$\gamma \cdot z = \frac{\alpha z + \beta}{\bar{\beta} z + \bar{\alpha}}, \quad z \in \mathcal{D} \tag{3}$$

Orientation reversing isometries of $\mathcal{D}$ are obtained by composing any transformation (3) with the reflexion $\kappa : z \to \bar{z}$. The full symmetry group of the Poincaré disc is therefore:

$$\mathrm{U}(1,1) = \mathrm{SU}(1,1) \cup \kappa \cdot \mathrm{SU}(1,1)$$

Transformations in $\mathrm{SU}(1,1)$ can be of three types: elliptic (those belong to the conjugacy class of usual rotations centered at the origin of the disc), parabolic (those have a unique fixed point which lies on the boundary of $\mathcal{D}$) and hyperbolic (two fixed points on $\partial\mathcal{D}$).

The octagonal lattice group Γ is generated by the following four hyperbolic transformations (boosts), see [5]:

$$g_0 = \begin{pmatrix} 1+\sqrt{2} & \sqrt{2+2\sqrt{2}} \\ \sqrt{2+2\sqrt{2}} & 1+\sqrt{2} \end{pmatrix} \tag{4}$$

and $g_j = r_{j\pi/4} g_0 r_{-j\pi/4}$, $j = 1, 2, 3$, where r_φ indicates the rotation of angle φ around the origin in $\mathcal{D}$. The fundamental domain of the lattice is a regular octagon $\mathcal{O}$ as shown in figure 1. The opposite sides of the octagon are identified by periodicity, so that the corresponding quotient surface $\mathcal{D}/\Gamma$ is isomorphic to a "double doughnut" (genus two surface) [5]. The fundamental octagon $\mathcal{O}$ can be further decomposed into 96 congruent triangles (see Figure 1) with angles $\pi/2$, $\pi/3$ and $\pi/8$. By applying reflections through the sides of one triangle (like the purple one in figure 1) and iterating the process, applying if necessary a translation in Γ to get the resulting triangle back to $\mathcal{O}$, one fills out the octagon. The set of all these transformations (mod Γ) is isomorphic to the group of automorphisms of $\mathcal{D}/\Gamma$, we call it $\mathcal{G}$. Let us call P, Q, R the vertices of the red triangle in Figure 1 which have angles $\pi/8$, $\pi/2$ and $\pi/3$ respectively.

Definition 1. *We set :*
(i) κ, κ' and κ'' the reflections through the sides PQ, PR and QR respectively (mod Γ);
(ii) ρ the rotation by $\pi/4$ centered at P, σ the rotation by π centered at Q and ϵ the rotation by $2\pi/3$ centered at R (mod Γ).

Note that $\rho = \kappa'\kappa$, $\sigma = \kappa''\kappa$ and $\epsilon = \kappa''\kappa'$. Moreover $\rho\sigma\epsilon = Id$. Any two of these "rotations" generate the subgroup $\mathcal{G}_0$ of orientation-preserving automorphisms of $\mathcal{G}$. It can be seen that $\mathcal{G} = \mathcal{G}_0 \cup \kappa \cdot \mathcal{G}_0$, and

moreover $\mathcal{G}_0$ can be identified with $GL(2,3)$, the group of invertible 2×2 matrices with entires in the field $\mathbb{Z}_3$.

Tables 1 and 2 list the conjugacy classes of elements in $\mathcal{G}_0$ and $\mathcal{G} \setminus \mathcal{G}_0$ respectively. In table 2 we

class number	1	2	3	4	5	6	7
representative	Id	ρ	ρ^2	$-Id$	σ	ϵ	$-\epsilon$
order	1	8	4	2	2	3	6
# elements	1	12	6	1	12	8	8

Table 1: Conjugacy classes of $\mathcal{G}$, orientation preserving transformations

class number	8	9	10	11	12	13
representative	κ	κ'	$\widehat{\sigma}\kappa$	$\rho\widehat{\sigma}\kappa$	$\epsilon\kappa$	$-\epsilon\kappa$
order	2	2	8	4	12	12
# elements	6	12	12	2	8	8

Table 2: Conjugacy classes of $\mathcal{G}$, orientation reversing transformations

simplify expressions by using the notation $\widehat{\sigma} = \epsilon\sigma\epsilon^{-1}$. We also define $\widetilde{\sigma} = \rho^2\sigma\rho^{-2}$. Note that $\widehat{\sigma}$ is the rotation by π centered at the point $\widehat{S}$ (mod Γ) and $\widetilde{\sigma}$ is the rotation by π centered at $\widetilde{S}$ (mod Γ) in figure 1.

There are 13 conjugacy classes and therefore 13 complex irreducible representations of $\mathcal{G}$, the characters of which will be denoted χ_j, $j = 1, ..., 13$. The character table, as computed by the group algebra software GAP is shown in table 3 (GAP, http://www.gap-system.org/). The character of the identity is equal to the dimension of the corresponding representation. It follows from table 3 that there are 4 irreducible representations of dimension 1, 2 of dimension 2, 4 of dimension 3 and 3 of dimension 4. In the following we shall denote the irreducible representations by their character: χ_j is the representation with this character. The following lemma is proved in [15].

Lemma 1. *All the irreducible representations of $\mathcal{G}$ are real absolutely irreducible. In other words, any matrix which commutes with such a representation is a real scalar multiple of the identity matrix.*

Class #	1	2	3	4	5	6	7	8	9	10	11	12	13
Representative	Id	ρ	ρ^2	$-Id$	σ	ϵ	$-\epsilon$	κ	κ'	$\widehat{\sigma}\kappa$	$\rho\widehat{\sigma}\kappa$	$\epsilon\kappa$	$-\epsilon\kappa$
χ_1	1	1	1	1	1	1	1	1	1	1	1	1	1
χ_2	1	-1	1	1	-1	1	1	1	-1	-1	1	1	1
χ_3	1	-1	1	1	-1	1	1	-1	1	1	-1	-1	-1
χ_4	1	1	1	1	1	1	1	-1	-1	-1	-1	-1	-1
χ_5	2	0	2	2	0	-1	-1	-2	0	0	-2	1	1
χ_6	2	0	2	2	0	-1	-1	2	0	0	2	-1	-1
χ_7	3	1	-1	3	-1	0	0	-1	-1	1	3	0	0
χ_8	3	1	-1	3	-1	0	0	1	1	-1	-3	0	0
χ_9	3	-1	-1	3	1	0	0	1	-1	1	-3	0	0
χ_{10}	3	-1	-1	3	1	0	0	-1	1	-1	3	0	0
χ_{11}	4	0	0	-4	0	-2	2	0	0	0	0	0	0
χ_{12}	4	0	0	-4	0	1	-1	0	0	0	0	$\sqrt{3}$	$-\sqrt{3}$
χ_{13}	4	0	0	-4	0	1	-1	0	0	0	0	$-\sqrt{3}$	$\sqrt{3}$

Table 3: Irreducible characters of $\mathcal{G}$

2.2 Steady-state bifurcations with $\mathcal{G}$ symmetry: earlier results

We shall assume throughout the paper that a center manifold reduction has been performed for a steady-state bifurcation problem with $\mathcal{G}$ symmetry like it can arise with Eq. (2) restricted to Γ-periodic patterns in $\mathcal{D}$ and where $I_{ext} = 0$ (no external input). This means that a linear stability analysis of the trivial solution has led to finding a critical parameter value μ_c at which, in the class of Γ-periodic functions, 0 is an eigenvalue of the linear part. The existence of such critical points is discussed in [15] and [14]. It is a generic fact that the corresponding eigenspace X be an irreducible representation space of $\mathcal{G}$, and any irreducible representation can be involved, depending on the form of the function w defined in the introduction in (2). Then the center manifold reduction brings down the initial problem to an ODE posed in X which is invariant under the action of the irreducible representation of $\mathcal{G}$ in X, see [25] for a complete and rigorous exposition of the method, and [12] for an exposition in the context of equivariant bifurcations.

Here it may be useful to recall some basic facts about bifurcations with symmetry. We write the bifurcation equation in X

$$\frac{dx}{dt} = \alpha(\lambda)\ x + f(x,\lambda) \tag{5}$$

where $\lambda = \mu - \mu_c$ and α is a real C^k function ($k \geq 1$) with $\alpha(0) = 0$, $f : X \times \mathbb{R} \to X$ has order $\|x\|o(\|x\|)$ and commutes with the action of $\mathcal{G}$ in X: if we denote by $(g, x) \mapsto g \cdot x$ the action (representation) of the group in X, then $f(g \cdot x, \lambda) = g \cdot f(x, \lambda)$ for all triples (g, x, λ). Moreover the property $\alpha'(0) \neq 0$ is generic and we shall assume it throughout the paper. We can even assume $\alpha'(0) > 0$ so that the trivial solution looses stability when $\lambda > 0$. This implies that after a suitable change of variable we can make the following hypothesis.

Hypothesis : $\alpha(\lambda) = \lambda$ in (5).

The problem is now to find the non trivial solutions $(x(\lambda), \lambda)$ of (5) such that $x(0) = 0$ and to analyze the nearby dynamics. Let H be an isotropy subgroup of $\mathcal{G}$: $H = \{g \in \mathcal{G} \mid g \cdot x = x\}$ for some point $x \in X$. We define the fixed point subspace of H, or subspace of H symmetry, as

$$X^H = \{x \in X \mid H \cdot x = x\}.$$

Then for all $h \in H$ we have that $h \cdot f(x, \lambda) = f(h \cdot x, \lambda) = f(x, \lambda)$. Hence X^H is invariant under the flow generated by (5): if $x(0) \in X^H$, then $x(t) \in X^H$ for all t. We shall later use the notation $\mathrm{Fix}(H)$ instead of X^H for convenience.

It follows that by restricting ourselves to the search of solutions with a given isotropy H, we just need to solve (5) in the fixed point subspace X^H. The case when $\dim X^H = 1$ is of particular interest. In this case looking for solutions with isotropy H reduces to solving a *scalar bifurcation equation*. Under the above assumptions, this equation always has a branch of non trivial, bifurcated equilibria. By group invariance of the problem any solution generates new solutions by letting $\mathcal{G}$ act on it. There is a one to one correspondance between the number of elements in this $\mathcal{G}$-orbit of solutions and the number of elements in the quotient $\mathcal{G}/H$ (number of subgroups conjugate to H in $\mathcal{G}$). We call the conjugacy class of an isotropy subgroup H the *isotropy type* of H.

Moreover, writing $N(H)$ the normalizer of H in $\mathcal{G}$, if $N(H)/H$ is trivial then generically this branch is transcritical: $x(\lambda) = O(|\lambda|)$, while if $N(H)/H \simeq \mathbb{Z}_2$, the branch is generically a *pitchfork*: $x(\lambda) = \pm O(\sqrt{|\lambda|})$.

The above results when $\dim X^H = 1$ are known as the *Equivariant Branching Lemma*, see [22], [12]. We may therefore say that if the hypotheses of the Equivariant Branching Lemma are satisfied for a subgroup H, then the isotropy type of H is symmetry-breaking.

Note that, when restricted to the invariant axis X^H as above, the *exchange of stability principle* holds for these solutions. Indeed let the axis of symmetry be parametrized by a real coordinate u, the equation on this axis at leading order has the form $\dot{u} = \lambda u + Cu^k$ where C is a real coefficient and $k \geq 2$. The bifurcated branch is parametrized (at leading order) by $\lambda = -Cu^{k-1}$, so that the radial eigenvalue is $(k-1)Cu^{k-1} = -(k-1)\lambda$ (at leading order). It therefore changes sign with λ. This eigenvalue is called *radial*. The other eigenvalues for the Jacobian matrix J of (5) evaluated at the solutions are *transverse* (the eigenvectors point orthogonally to the axis of symmetry). The bifurcated equilibria are stable in X if the eigenvalues of J have all a negative real part. The exchange of stability principle does not hold in general when considering stability in the full space X.

Equilibria with isotropy not satisfying the condition $\dim X^H = 1$ or other types of bounded solutions may also exist, however their analysis requires a knowledge of the *equivariant structure* of the vector field f or at least of its Taylor expansion up to an order large enough to fully determine the bifurcation diagram. We shall see in the next sections that solving the bifurcation equation (5) when $\dim X = 4$ requires computing the equivariant terms in the expansion of $f(\cdot, \lambda)$ up to order 3 in certain cases, up to order 5 or even 7 in another case.

We now come back to our specific problem with $\mathcal{G}$ symmetry. We can see from the character table 3 that there are 13 possible cases for the irreducible representations. The dimension of X for each representation χ_j $(j = 1, \ldots, 13)$ is given by the corresponding character evaluated at the identity. We see that $\dim(X) = 1$ for $\chi_1, \ldots, \chi_4$, $\dim(X) = 2$ for χ_5, χ_6, $\dim(X) = 3$ for $\chi_7, \ldots, \chi_{10}$ and $\dim(X) = 4$ for χ_{11}, χ_{12} and χ_{13}. In order to give an exhaustive description of the bifurcation diagrams with $\mathcal{G}$ symmetry we have to consider all these 13 cases.

For the representations χ_1 to χ_{10} in Table 3, it has been established in [15] that the bifurcation diagrams are identical to those of classical bifurcation problems with symmetry in $\mathbb{R}$, $\mathbb{R}^2$ or $\mathbb{R}^3$. Let us summarize these cases in the following theorem. The word "natural" for a group representation means that the action is that of the group itself as a matrix group.

Theorem 1. *For generic steady-state bifurcation diagrams with $\mathcal{G}$ symmetry the following holds.*

(i) χ_1*: transcritical bifurcation (trivial symmetry, exchange of stability holds);*

(ii) χ_2, χ_3, χ_4*: pitchfork bifurcation ($\mathbb{Z}_2$ symmetry, exchange of stability holds);*

(iii) χ_5*: same as bifurcation with natural hexagonal D_6 symmetry in the plane;*

(iv) χ_6*: same as bifurcation with natural triangular D_3 symmetry in the plane;*

(v) χ_7*: same as bifurcation with natural octahedral $\mathbb{O}$ symmetry in $\mathbb{R}^3$;*

(vi) χ_{10}*: same as bifurcation with the (unique) non natural octahedral symmetry in $\mathbb{R}^3$;*

(vii) χ_8*: same as bifurcation with natural full octahedral $\mathbb{O} \ltimes \mathbb{Z}_2$ symmetry in $\mathbb{R}^3$;*

(viii) χ_9*: same as bifurcation with the (unique) non natural full octahedral symmetry in $\mathbb{R}^3$.*

Moreover in all cases, bifurcated solutions satisfy the Equivariant Branching Lemma and their isotropies are listed in Theorem 5 of [15].

Theorem 5 of [15] gives also the isotropy types of representations χ_{11}, χ_{12} and χ_{13} which have one dimensional fixed-point subspace. Hence by application of the Equivariant Branching Lemma, we know that branches of solutions with these isotropies exist (in a generic sense). However bifurcation diagrams cannot be deduced from already known bifurcation problems. Our aim in the remainder of this paper is to fill this gap. In the next proposition we list these isotropy subgroups which give bifurcated solutions by the Equivariant Branching Lemma. We introduce the following subgroups which will be relevant in the remainder of the paper. We use the notation $\widetilde{\sigma} = \rho^2 \sigma \rho^{-2}$ (see Table 1).

Definition 2.

$$\begin{aligned}
\widetilde{C}_{2\kappa} &= \langle \sigma, \kappa \rangle = \{Id, \sigma, \kappa, \kappa''\} \\
\widetilde{C}'_{2\kappa} &= \langle \widetilde{\sigma}, \kappa \rangle = \{Id, \tilde{\sigma}, \kappa, -\rho^2 \kappa'' \rho^{-2}\} \\
\widetilde{C}_{3\kappa'} &= \langle \epsilon, \kappa' \rangle = \{Id, \epsilon, \epsilon^2, \kappa', \epsilon\kappa'\epsilon^2, \epsilon^2\kappa'\epsilon\} \\
\widetilde{D}_3 &= \langle \widetilde{\sigma}, \epsilon \rangle = \{Id, \epsilon, \epsilon^2, \widetilde{\sigma}, \epsilon\widetilde{\sigma}\epsilon^2, \epsilon^2\widetilde{\sigma}\epsilon\}
\end{aligned}$$

Proposition 1. *For the 4D representations of $\mathcal{G}$, the isotropy subgroups with one dimensional fixed point subspace are the following:*

- χ_{11}*:* $\widetilde{C}_{2\kappa}$, $\widetilde{C}'_{2\kappa}$*;*
- χ_{12}*:* $\widetilde{D}_3$, $\widetilde{C}_{3\kappa'}$, $\widetilde{C}_{2\kappa}$, $\widetilde{C}'_{2\kappa}$*;*
- χ_{13}*:* $\widetilde{D}_3$, $\widetilde{C}_{3\kappa'}$, $\widetilde{C}_{2\kappa}$, $\widetilde{C}'_{2\kappa}$.

These isotropy types are therefore symmetry-breaking.

2.3 Octagonal H-planforms

In the last section of [15], we tackled the problem of computing octagonal H-planforms and we described numerical and geometrical methods to achieve this study. We recall that these planforms are eigenfunctions of the Laplace-Beltrami operator in $\mathcal{D}$ which satisfy certain isotropy conditions: (i) being invariant under a lattice group Γ and (ii) being invariant under the action of an isotropy subgroup of the symmetry group of the fundamental domain $\mathcal{D}/\Gamma$ (mod Γ).

Lemma 2. *The Laplace-Beltrami operator in $\mathcal{D}$ in z_1, z_2 coordinates is*

$$\Delta_{\mathcal{D}} = \frac{(1 - z_1^2 - z_2^2)^2}{4} \left[\frac{\partial^2}{\partial z_1^2} + \frac{\partial^2}{\partial z_2^2} \right] \text{ for } z = z_1 + \mathbf{i} z_2 \in \mathcal{D}$$

The computations of the four planforms associated to the one-dimensional irreductible representations have been performed using the finite element method (see [16] for a review) on "desymmetrized" domains of the hyperbolic octagon with a mixture of Dirichlet and Neumann boundary conditions as it is used in [5, 4, 40]. The principles of desymmetrization in the context of dihedral symmetry can be found in the book of Fässler and Stiefel [18]. For the two and three dimensional representations, we implemented the finite element method with periodic boundary conditions in the octagon and identified a posteriori the corresponding planforms. In this section, we complete this study for the four-dimensional case and we illustrate it with a selection of images of octagonal H-planforms.

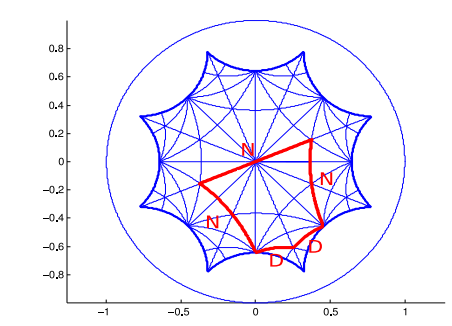

(a) $\widetilde{C}_{3\kappa'}$

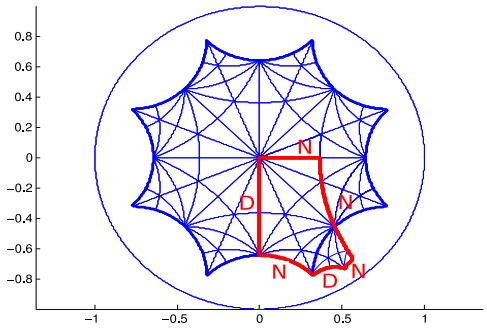

(b) $\widetilde{C}_{2\kappa}$

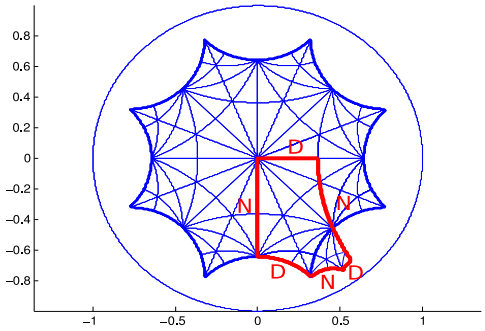

(c) $\overline{C}'_{2\kappa}$

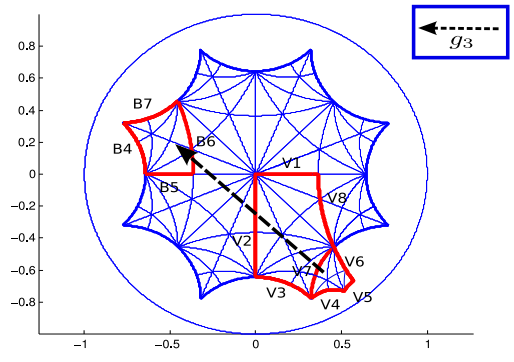

(d) Action of the boost g_3 on the desymmetrized domain corresponding to isotropy groups $\widetilde{C}_{2\kappa}$ and $\overline{C}'_{2\kappa}$, see text.

Figure 2: Desymmetrized domain in red and associated boundary conditions corresponding to isotropy groups $\widetilde{C}_{3\kappa'}$, $\widetilde{C}_{2\kappa}$ and $\overline{C}'_{2\kappa}$. Letters N and D mean respectively Neumann and Dirichlet boundary conditions.

We first explain how to recover the desymmetrized domain and the associated boundary conditions for isotropy group $\widetilde{C}_{3\kappa'}$ in figure 2(a). The group $\widetilde{C}_{3\kappa'}$ has six elements among them: ϵ the rotation by $2\pi/3$ centered at R, κ' and κ'' the reflections through the side PR and QR respetively, where P, Q and R are the vertices of the purple triangle in figure 1. Each reflections imply Neumann boundary conditions on their respective edges. The Dirichlet boundary conditions prevent an additional 3-fold rotation. The last Neumann boundary condition is obtained by translating the desymmetrized domain with the four boosts (4).

In order to better illustrate the intrinsic differences of planforms with isotropy types $\widetilde{C}_{2\kappa}$ and $\widetilde{C}'_{2\kappa}$, we decide to work with $\overline{C}'_{2\kappa} = \{Id, -\sigma, -\kappa, \kappa''\}$, a conjugate of $\widetilde{C}'_{2\kappa}$. Indeed, isotropy groups $\widetilde{C}_{2\kappa}$ and $\overline{C}'_{2\kappa}$ share the same desymmetrized domain but have different boundary conditions depending on their symmetries, see figure 2(b) and 2(c). As we apply finite element method to compute the eigenvalues and eigenvectors of the Laplace-Beltrami operator, it is more convenient to work with connected domain. This is why the desymmetrized domain of isotropy groups $\widetilde{C}_{2\kappa}$ and $\overline{C}'_{2\kappa}$ has the particularity to have a part outside the octagon, however by the action of the boost g_3 one can translate this part inside the octagon, see figure 2(d). Indeed, domain delimited by edges $V4 - V5 - V6 - V7$ is translated into the domain delimited by edges $B4 - B5 - B6 - B7$ by the boost g_3. For isotropy group $\widetilde{C}_{2\kappa}$, the reflections κ and κ'' impose Neumann boundary condition on edges $V1, B5$ and $V8, V6$ respectively and the action of g_3^{-1} implies Neumann boundary condition on edge $V5 = g_3^{-1}(B5)$. We have to impose Dirichlet boundary condition on edge $V2$ to prevent the action of $-\kappa$, which does not belong $\widetilde{C}_{2\kappa}$, and this further implies Dirichlet condition on $B4$ and thus on $V4$. Finally, reflection κ combined with boost g_2 (g_2 translates edge $V3$ to the opposite side of the octagon) gives Neumann boundary condition on edge $V3$. Same method applies to isotropy group $\overline{C}'_{2\kappa}$ and we find the boundary conditions presented in figure 2(c). For isotropy group $\widetilde{D}_3$, we do not find any simple desymmetrized domain as in the other cases and we use the finite element method on the full octagon with periodic boundary conditions: opposite sides of the octagon are identified by periodicity. To identify planforms with isotropy group $\widetilde{D}_3$, we first select eigenvectors with eigenfunctions of multiplicity 4 and then check the symmetries.

We show in figure 3 four H-planforms with isotropy groups $\widetilde{C}_{2\kappa}$, $\overline{C}'_{2\kappa}$, $\widetilde{C}_{3\kappa'}$ and $\widetilde{D}_3$ with eigenvalue $\lambda = 5.3537$ and in figure 4 two H-planforms with isotropy groups $\widetilde{C}_{2\kappa}$, $\overline{C}'_{2\kappa}$. Planform with isotropy group $\widetilde{D}_3$ is the only one which does not possess any reflection, it is then easy to distinguish it from other planforms, see figure 3(d). We notice that patterns of planforms with isotropy $\widetilde{C}_{2\kappa}$, figure 3(a), and $\widetilde{C}_{3\kappa'}$, figure 3(c), seem to be similar, up to a rotation, despite the two cooresponding groups are different. On the contrary, it is easy to distinguish patterns of groups $\widetilde{C}_{2\kappa}$, figures 3(a) and 4(a), and $\overline{C}'_{2\kappa}$, figures 3(b) and 4(b).

In figures 3 and 4, we have plotted for convenience, the corresponding H-planforms in the octagon only. Nevertheless, H-planforms are periodic in the Poincaré disk and in figure 5, we plot the H-planform with $\widetilde{C}_{3\kappa'}$ isotropy type of figure 3(c). As the octagonal lattice group Γ is generated by the four boosts of equation (4), then once an H-planform is computed, we report it periodically in the whole Poincaré disk by the action of these boosts and obtain figure 5.

2.4 Bifurcation with submaximal isotropy

The condition $\dim X^H = 1$, required by the Equivariant Branching Lemma, implies that H is *maximal* (there no isotropy subgroup between H and $\mathcal{G}$). However it is well-known that solutions with non maximal isotropy can occur in generic bifurcation problems. It follows that the Equivariant Branching Lemma does not account for all the bifurcating equilibria and that the study of bifurcation with *submaximal* isotropy is an important issue. Here we adopt the approach of [13], see also [12]

We briefly recall some basic results on bifurcation with submaximal isotropy. The key for such an analysis is the determination of the number of copies in $\mathrm{Fix}(\Sigma)$ of subspaces $\mathrm{Fix}(\Delta)$ for the isotropy subgroups Δ containing Σ. Let $[\Sigma]$ be the conjugacy classe of Σ and write $[\Sigma] < [\Delta]$ if only if $[\Sigma] \neq [\Delta]$ and $\gamma^{-1}\Sigma\gamma \subset \Delta$ for some $\gamma \in \mathcal{G}$. We call *isotropy type* the conjugacy class of an isotropy subgroup. Let $[\Delta_1], \ldots, [\Delta_r]$ be the isotropy types which satisfy the former condition. Let a_j the number of solution branches with isotropy Δ_j (a_j may be equal to 0). Then the total number of nontrivial solution branches

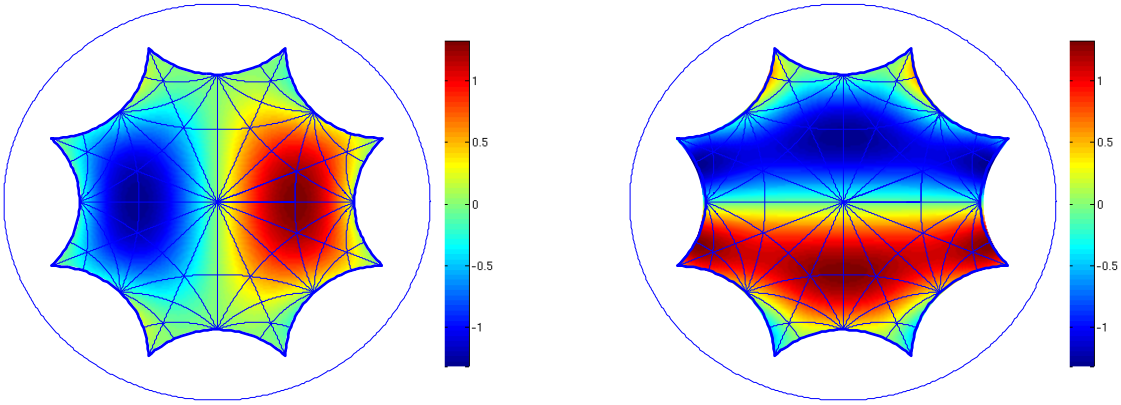

(a) $\widetilde{C}_{2\kappa}$ (b) $\overline{C}'_{2\kappa}$

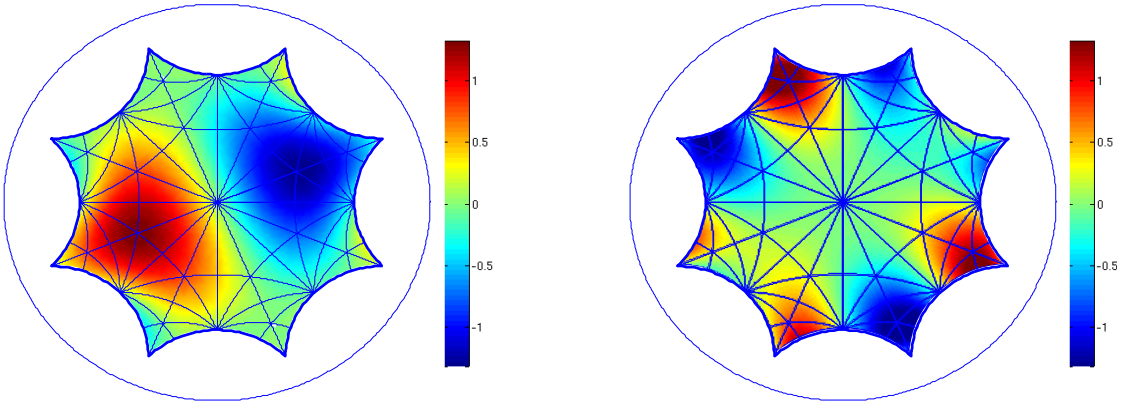

(c) $\widetilde{C}_{3\kappa'}$ (d) $\widetilde{D}_3$

Figure 3: The four H-planforms associated to the eigenvalue $\lambda = 5.3537$.

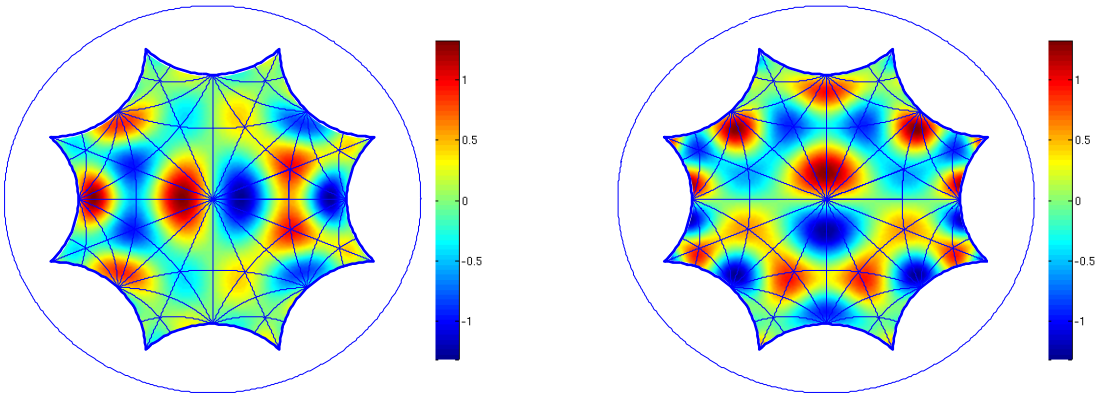

(a) $\widetilde{C}_{2\kappa}$ (b) $\overline{C}'_{2\kappa}$

Figure 4: Two H-planforms corresponding to isotropy group $\widetilde{C}_{2\kappa}$ right and $\overline{C}'_{2\kappa}$ left for eigenvalue $\lambda = 42.3695$.

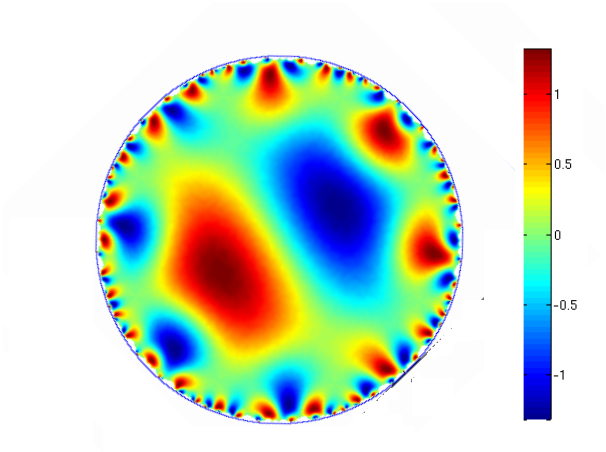

Figure 5: Extension of the $\widetilde{C}_{3\kappa'}$ H-planform on the Poincaré disk of figure 3(c).

in $\mathrm{Fix}(\Sigma)$ with higher isotropy is

$$N^{\Sigma} = \sum_{j=1}^{r} a_j n(\Sigma, \Delta_j)$$

where $n(\Sigma, \Delta_j)$ is the number of conjugate copies of $\mathrm{Fix}(\Delta)$ inside $\mathrm{Fix}(\Sigma)$.

We denote by f^{Σ} the restriction to $\mathrm{Fix}(\Sigma)$ of f given by in Eq. (5). Then, if f^{Σ} has N^0 zeroes in a neighborhood of the origin, there are precisely $N^0 - N^{\Sigma} - 1$ branches of equilibria with isotropy Σ.

If we set $N(\Sigma) = \{g \in \mathcal{G} \mid g^{-1}\Sigma g = \Sigma\}$ (normalizer of Σ in $\mathcal{G}$) and $N(\Sigma, \Delta) = \{g \in \mathcal{G} \mid \Sigma \subset g\Delta g^{-1}\}$, the quotient set $\dfrac{N(\Sigma, \Delta)}{N(\Delta)}$ is well-defined even though $N(\Sigma, \Delta)$ is not a group in general [13]. Moreover we have that

$$n(\Sigma, \Delta) = \left| \frac{N(\Sigma, \Delta)}{N(\Delta)} \right|$$

This formula allow us to compute the numbers $n(\Sigma, \Delta)$, hence to determine the number of solutions with isotropy Δ in $\mathrm{Fix}(\Sigma)$.

Now note that the maximal isotropy subgroups for the representations χ_{11}, χ_{12} and χ_{13} which are listed in Definition 2, have only cyclic subgroups generated by elements σ, ϵ, κ or κ' (or conjugates). The following lemmas give the informations when Δ is maximal.

Lemma 3. *The normalizers of the isotropy subgroups of proposition 1 are listed in table 4.*

Δ	$N(\Delta)$	$\lvert N(\Delta)\rvert$
$\widetilde{D}_3$	$\langle \widetilde{D}_3, -Id \rangle$	12
$\widetilde{C}_{3\kappa'}$	$\langle \widetilde{C}_{3\kappa'}, -Id \rangle$	12
$\widetilde{C}_{2k}$	$\langle \widetilde{C}_{2k}, -Id \rangle$	8
$\widetilde{C}'_{2\kappa}$	$\langle \widetilde{C}'_{2\kappa}, -Id \rangle$	8

Table 4: Isotropy subgroups of $\mathcal{G}$ and their normalizer. The last column provides the cardinal of the normalizer.

Proof. Let us consider, for example, $\Sigma = \widetilde{C}_{2k} = \langle \sigma, \kappa \rangle$. The only conjugate of κ in $\widetilde{C}_{2k}$ is κ itself, and the same holds for σ and $\sigma\kappa = \kappa'$. Therefore $N(\widetilde{C}_{2k}) = N(\langle\kappa\rangle) \cap N(\langle\sigma\rangle) \cap N(\langle\sigma\kappa\rangle)$. Now for any element $h \in \mathcal{G}$, we have that $|N(\langle h \rangle)| = \frac{96}{|[h]|}$. Tables 1 and 2 show that $|[\kappa]| = 6$ while $|[\sigma]| = |[\kappa']| = 12$. It follows that $|N(\langle\kappa\rangle)| = 16$ while $|N(\langle\sigma\rangle)| = |N(\langle\kappa'\rangle)| = 8$. Hence $|N(\Sigma)| \leq 8$. But $\Sigma \subset N(\Sigma)$ and $|\Sigma| = 4$, moreover $-Id$ commutes with any element in $\mathcal{G}$ and therefore belongs to $N(\Sigma)$. It follows that the group $\langle \Sigma, -Id \rangle = N(\Sigma)$. The same rationale applies to the other isotropy subgroups. □

Lemma 4. *The values of $n(\Sigma, \Delta)$ for the maximal isotropy subgroups Δ (see Definition 2) are given in table 5.*

$[\Sigma]$	$[\Delta]$	$n(\Sigma, \Delta)$
$\langle\sigma\rangle$	$\widetilde{C}_{2k}$	1
$\langle\sigma\rangle$	$\widetilde{C}'_{2k}$	1
$\langle\sigma\rangle$	$\widetilde{D}_3$	2
$\langle\epsilon\rangle$	$\widetilde{D}_3$	2
$\langle\epsilon\rangle$	$\widetilde{C}_{3\kappa'}$	2
$\langle\kappa\rangle$	$\widetilde{C}_{2k}$	2
$\langle\kappa\rangle$	$\widetilde{C}'_{2\kappa}$	2
$\langle\kappa'\rangle$	$\widetilde{C}_{2\kappa}$	1
$\langle\kappa'\rangle$	$\widetilde{C}'_{2\kappa}$	1
$\langle\kappa'\rangle$	$\widetilde{C}_{3\kappa'}$	2

Table 5: Values of $n(\Sigma, \Delta)$.

Proof.

- Case $\Sigma = \langle\kappa\rangle$: we have $N(\Sigma, \widetilde{C}_{2k}) = N(\Sigma, \widetilde{C}'_{2k}) = N(\Sigma)$ as κ is not conjugate to σ nor to $\sigma\kappa$. Moreover, $|N(\Sigma)| = 16$ (see proof of Lemma 3) and $|N(\widetilde{C}_{2k})| = |N(\widetilde{C}'_{2k})| = 8$, hence $n(\Sigma, \widetilde{C}_{2k}) = n(\Sigma, \widetilde{C}'_{2k}) = 2$.
- Case $\Sigma = \langle\sigma\rangle$: we have $N(\Sigma, \widehat{C}_{2k}) = N(\Sigma, \widetilde{C}'_{2k}) = N(\Sigma)$ with $|N(\Sigma)| = 8$ (see proof of Lemma 3), hence $n(\Sigma, \widehat{C}_{2k}) = n(\Sigma, \widetilde{C}'_{2k}) = 1$. By definition $N(\Sigma, \widetilde{D}_3) = \{g \in \mathcal{G} \mid g\Sigma g^{-1} \subset \widetilde{D}_3\} = \{g \in \mathcal{G} \mid g\widetilde{\sigma}g^{-1} \in \widetilde{D}_3\}$. There are three conjugates of $\widetilde{\sigma}$ in $\widetilde{D}_3$. Therefore $|N(\Sigma, \widetilde{D}_3)| = 3|N(\langle\sigma\rangle)|$. As shown in the proof of Lemma 3), $|N(\langle\sigma\rangle)| = 8$, hence $N(\Sigma, \widetilde{D}_3) = 24$ and $n(\Sigma, \widetilde{D}_3) = 2$.
- The proof for the other cases uses the same arguments as above.

□

3 Bifurcation diagrams in the case of the representation χ_{12}

The character table 3 shows that the two 4D representations χ_{12} and χ_{13} are almost identical, the only difference coming from the fact that the characters of the group elements $\epsilon\kappa$ and $-\epsilon\kappa$ have opposite signs. It follows that the general bifurcation analysis in the case of χ_{13} is identical to the case of χ_{12} and does not introduce any novelty. In the following we shall therefore only describe the χ_{12} case.

3.1 Equivariant structure of the equations on the center manifold

We need to know the form of the asymptotic expansion of the $\mathcal{G}$ equivariant map $f(\cdot, \lambda)$ in Equation (5). The dimension of the space of equivariant polynomials can be computed using Molien series (see [12]). This computation is shown in appendix B and the results are presented in table 15. The Molien series tells us that there are two independant equivariant homogeneous polynomial maps of order 3. The computation of these terms will prove to be sufficient to fully determine the bifurcation diagram under generic conditions.

We first need to choose a system of coordinates in $\mathbb{R}^4$. In the remaining part of this paper we shall use the same notation for an element in $\mathcal{G}$ and for its representation when there is no ambiguity. The following lemma is proved in Appendix C.1.

Lemma 5. *For the representation χ_{12} the diagonalization of the 8-fold symmetry matrix ρ has the form*

$$\rho = \begin{bmatrix} \exp(\frac{\mathbf{i}\pi}{4}) & 0 & 0 & 0 \\ 0 & \exp(-\frac{\mathbf{i}\pi}{4}) & 0 & 0 \\ 0 & 0 & \exp(\frac{3\mathbf{i}\pi}{4}) & 0 \\ 0 & 0 & 0 & \exp(-\frac{3\mathbf{i}\pi}{4}) \end{bmatrix}$$

We note $(z_1, \bar{z}_1, z_2, \bar{z}_2)$ *the complex coordinates in the corresponding basis.*

The following theorem gives the form of the bifurcation equations on the center manifold .

Theorem 2. *For the representation* χ_{12}*, Equation* (5) *expressed in the coordinates* $(z_1, \bar{z}_1, z_2, \bar{z}_2)$ *admits the following expansion*

$$\dot{z}_1 = \left[\lambda + a(|z_1|^2 + |z_2|^2)\right] z_1 + b\left[\sqrt{3}\left(3z_1^2 + \bar{z}_2^2\right)\bar{z}_1 - \mathbf{i}\left(z_2^2 + 3\bar{z}_1^2\right) z_2\right] + h.o.t. \tag{6}$$

$$\dot{z}_2 = \left[\lambda + a(|z_1|^2 + |z_2|^2)\right] z_2 + b\left[\sqrt{3}\left(3z_2^2 + \bar{z}_1^2\right)\bar{z}_2 + \mathbf{i}\left(z_1^2 + 3\bar{z}_2^2\right) z_1\right] + h.o.t. \tag{7}$$

where $(a, b) \in \mathbb{R}^2$*. Moreover the cubic part is the gradient of the* $\mathcal{G}$ *invariant real polynomial function*

$$\frac{a}{2}\left[\left(|z_1|^2 + |z_2|^2\right)^2\right] + b \cdot \left[\frac{\sqrt{3}}{2}\left(3\left(z_1^2\bar{z}_1^2 + z_2^2\bar{z}_2^2\right) + z_1^2 z_2^2 + \bar{z}_1^2\bar{z}_2^2\right) + \mathbf{i}\left(z_1^3\bar{z}_2 + \bar{z}_2^3 z_1 - z_2^3\bar{z}_1 - z_2\bar{z}_1^3\right)\right]$$

Proof. We postpone to appendix C.1 the computation of the two cubic equivariant maps. The check of the gradient form is straightforward. □

3.2 Isotropy types and fixed points subspaces

Lemma 6. *The lattice of isotropy types for the representation* χ_{12} *is shown in Figure 6. The numbers in parentheses indicate the dimension of corresponding fixed-point subspaces.*

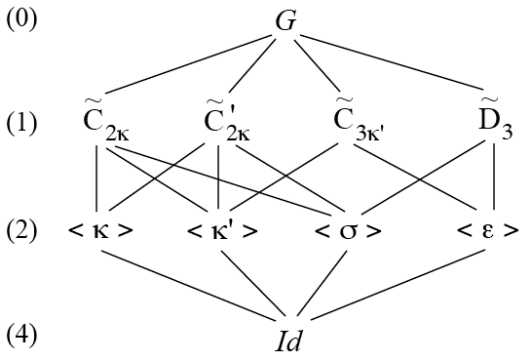

Figure 6: The lattice of isotropy types for the representation χ_{12}.

Proof. We apply the *trace formula*: if H is a subgroup and χ is the character of the representation, then

$$\dim(X^H) = \frac{1}{|H|}\sum_{h\in H}\chi(h) \tag{8}$$

By applying (8) for χ_{12} (see Table 3), one finds that the only cyclic subgroups of $\mathcal{G}$ (subgroups generated by one element) with a fixed-point subspace of positive dimension are those listed in the diagram of Figure 6, and this dimension is equal to 2. The result follows. Note that the isotropy types with one-dimensional fixed-point subspace have been determined in [15], see Proposition 1. □

The next lemma gives expressions for the fixed-point subspaces of two-element groups in the $(z_1, \bar{z}_1, z_2, \bar{z}_2)$ coordinates, which will be usefull for the bifurcation analysis of (5) in the planes of symmetry. There are four types of these planes but we express the fixed-point planes for the conjugates $\tilde{\sigma}$ of σ and κ'' of κ' for later convenience.

Lemma 7. *Fixed-point subspaces associated with the isotropy groups in the diagram 6 have the following equations.*

- $Fix(\sigma) = \{(z_1, \bar{z}_1, z_2, \bar{z}_2) \mid z_2 = (1-\sqrt{2})(\sqrt{2}z_1 - \mathbf{i}\sqrt{3}\bar{z}_1)\}$;
- $Fix(\tilde{\sigma}) = \rho^2 Fix(\sigma) = \{(z_1, \bar{z}_1, z_2, \bar{z}_2) \mid z_2 = (1-\sqrt{2})(\sqrt{2}z_1 + \mathbf{i}\sqrt{3}\bar{z}_1)\}$;
- $Fix(\epsilon) = \{(z_1, \bar{z}_1, z_2, \bar{z}_2) \mid z_2 = (1+\mathbf{i})z_1 + \sqrt{3}\bar{z}_1\}$;
- $Fix(\kappa) = \{(z_1, \bar{z}_1, z_2, \bar{z}_2) \mid z_1 = \mathbf{i}\bar{z}_1 \text{ and } z_2 = \mathbf{i}\bar{z}_2\}$;
- $Fix(\kappa') = \{(z_1, \bar{z}_1, z_2, \bar{z}_2) \mid \sqrt{2}z_1 = (-1+\mathbf{i})\bar{z}_1)\} \text{ and } \sqrt{2}z_2 = -(1+\mathbf{i})\bar{z}_2)\}$.
- $Fix(\kappa'') = \{(z_1, \bar{z}_1, z_2, \bar{z}_2) \mid z_2 = (\sqrt{3}-\sqrt{2})(-\sqrt{2}z_1 + \mathbf{i}\bar{z}_1)\}$.

Proof. Given in Appendix D.1. □

The one dimensional fixed point subspaces are the intersections of planes of symmetry. This allows to easily obtain expressions for these axes from the expressions listed in Lemma 7. For example we can write

$$\mathrm{Fix}(\widetilde{C}_{2\kappa}) = \{(z_1, z_2) \in \mathbb{C}^2 \mid z_1 = \mathbf{i}\bar{z}_1 \text{ and } z_2 = (1-\sqrt{2})(\sqrt{3}-\sqrt{2})z_1\}.$$

3.3 Bifurcation analysis

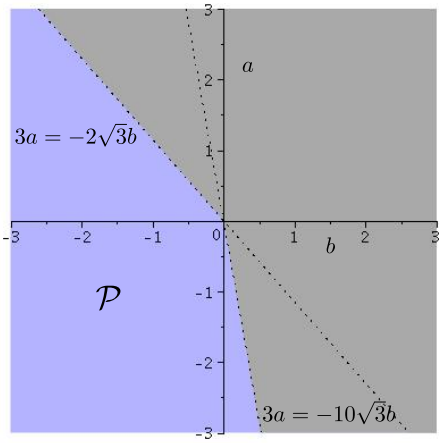

Figure 7: Region $\mathcal{P} = \{(a,b) \in \mathbb{R}^2 \mid 3a + 2b\sqrt{3} < 0 \text{ and } 3a + 10b\sqrt{3} < 0\}$ for the value of the parameters (a,b) is colored in blue.

Theorem 3. *Provided that* $(a,b) \in \mathcal{P} = \{(a,b) \in \mathbb{R}^2 \mid 3a + 2b\sqrt{3} < 0$ *and* $3a + 10b\sqrt{3} < 0\}$ *(see figure 7), the following holds for Equations (6)-(7).*

(i) No solution with submaximal isotropy bifurcates in the planes of symmetry.

(ii) The branches of equilibria with maximal isotropy (as listed in Proposition 1) are pitchfork and supercritical.

(iii) If $b > 0$ *(resp.* $b < 0$*), the equilibria with isotropy type* $\widetilde{C}_{3\kappa'}$ *(resp.* $\widetilde{D}_3$*) are stable in* $\mathbb{R}^4$*. Branches with isotropy* $\widetilde{C}_{2\kappa}$ *and* $\widetilde{C}'_{2\kappa}$ *are always saddles.*

Bifurcation diagrams restricted to the planes of symmetry are summerized in figure 8 in the case $b < 0$.

Remark 1. *We have numerically checked that the domain* $\mathcal{P}$ *coincides with the existence of an attracting, flow invariant sphere homeomorphic to* S^3 *in* $\mathbb{R}^4$*. By a theorem due to Field [19, 12], a condition for the existence of such a sphere is that* $\langle q(\xi), \xi \rangle < 0$ *for all* $\xi \neq 0$*, where* $\xi = (z_1, \bar{z}_1, z_2, \bar{z}_2)$*,* q *is the cubic part in the equations (6), (7) and* $\langle\ ,\ \rangle < 0$ *denotes the inner product* $\Re(z_1\bar{z}'_1 + z_2\bar{z}'_2)$*. Since* q *is an homogeneous polynomial map, it is sufficient to check the condition for* $(z_1, z_2) \in S^3$*, which does not present any difficulty.*

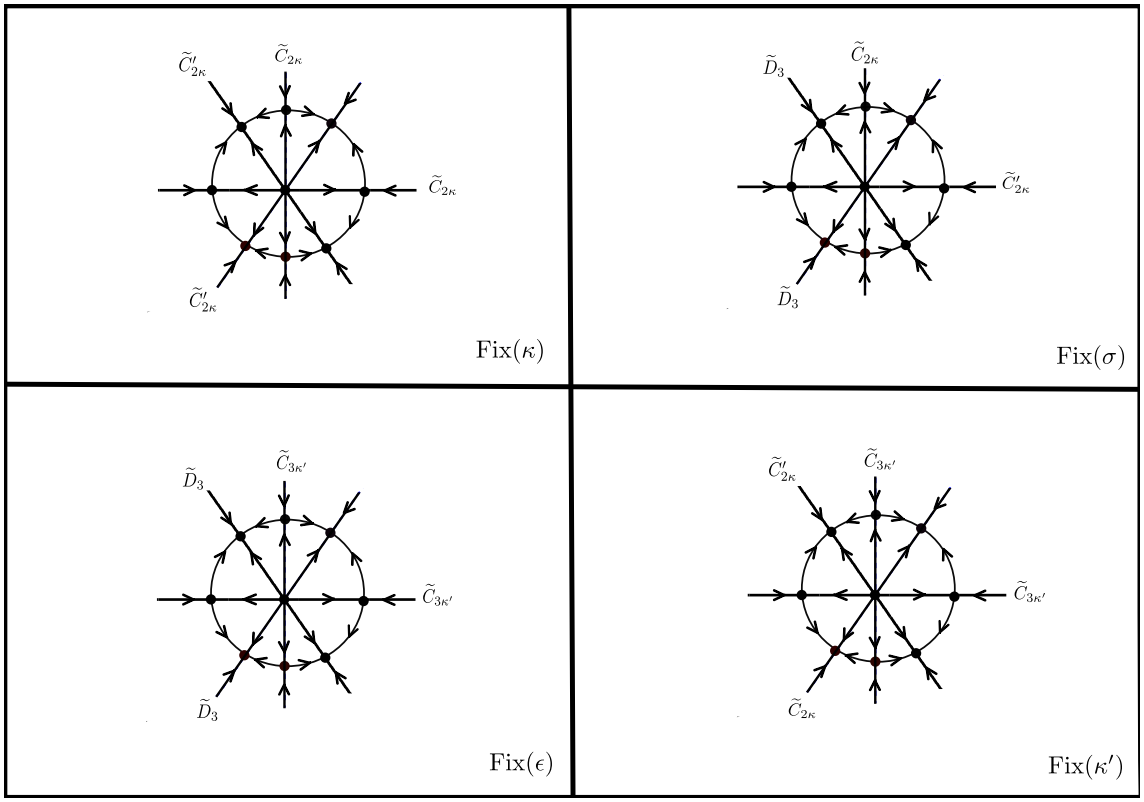

Figure 8: Bifurcation diagram in the case $b < 0$. For $b > 0$ the "non radial" arrows are reversed

Remark 2. *The theorem doesn't rule out the possibility that equilibria with trivial isotropy could bifurcate. We conjecture this is not the case. This is supported by the fact that under the "generic" hypotheses of the theorem: (i) no other solution than those with maximal isotropy bifurcates in the planes of symmetry, (ii) the stability of these solutions is determined at cubic order and one of these types is always stable, (iii) the system is gradient at cubic order, (iv) admitting the existence of an invariant sphere (previous remark), the conjecture doesn't contradict Poincaré-Hopf formula [24]: one can check that the sum of indices of equilibria with maximal isotropy is equal to 0, the Euler characteristic of S^3.*

Proof. We first examine bifurcation in the invariant planes. We can already note that, since $-Id$ acts non trivially in $\mathbb{R}^4 - \{0\}$ for χ_{12}, equilibria have to occur via pitchork bifurcations.
1. Bifurcation in the planes of symmetry. In each of the planes of symmetry there are precisely 4 axes of symmetry. This immediately follows from Table 5. For example Fix($\langle\sigma\rangle$) contains one copy of Fix($\widetilde{C}_{2\kappa}$), one copy of Fix($\widetilde{C}'_{2\kappa}$) and two copies of Fix($\widetilde{D}_3$). Let us choose real coordinates (x, y) in a plane of symmetry P and write the equations in P

$$\dot{x} = \lambda x + q_1(x, y) + h.o.t. \tag{9}$$
$$\dot{y} = \lambda y + q_2(x, y) + h.o.t. \tag{10}$$

where q_1 and q_2 are the components of the cubic part in the Taylor expansion of f restricted to P. If $(x(\lambda), y(\lambda))$ is a branch of equilibria of this system, then the equation

$$Q(x, y) = yq_1(x, y) - xq_2(x, y) = 0 \tag{11}$$

admits an axis of solutions $\epsilon(x_0, y_0)$ where (x_0, y_0) represents the leading order in the Taylor expansion of the solution. If Q is not degenerate the number of such axes is bounded by the degree of Q which is equal to 4. Now, there are 4 axes of symmetry in P and each of them corresponds to an axis of solutions of the above equation. Therefore if Q is not degenerate, there are no other invariant axes for Equation (11). To prove that there are no submaximal branches of solutions in the planes of symmetry it remains to check the non degeneracy of Q.

The stability of the bifurcated equilibria in the flow invariant planes is determined by the sign of the eigenvalues of the Jacobian matrix $\begin{pmatrix} \partial_x \dot{x} & \partial_y \dot{x} \\ \partial_x \dot{y} & \partial_y \dot{y} \end{pmatrix}$ evaluated at the equilibria. One eigenvalue is radial with leading part -2λ (since q_1 and q_2 are cubic), the other one is transverse (see Section 2.2). Bifurcation of an equilibrium is supercritical iff its radial eigenvalue is negative.

1. *Bifurcation and stability in* Fix(κ). By Lemma 7,

$$\mathrm{Fix}(\kappa) = \{(z_1, z_2) \in \mathbb{C}^2 | z_1 = (1+\mathbf{i})x \text{ and } z_2 = (1+\mathbf{i})y, \quad (x,y) \in \mathbb{R}^2\} \ .$$

By Table 5 this plane contains two axes with isotropy type $\widetilde{C}_{2\kappa}$ and two axes with isotropy type $\widetilde{C}_{2\kappa}$. We can choose as representatives $\mathrm{Fix}(\widetilde{C}_{2\kappa}) = \{y = (1-\sqrt{2})(\sqrt{3}-\sqrt{2})x\}$ and $\mathrm{Fix}(\widetilde{C}'_{2\kappa}) = \{y = (1-\sqrt{2})(\sqrt{3}+\sqrt{2})x\}$. We change coordinates so that $\mathrm{Fix}(\widetilde{C}_{2\kappa})$ is the real axis. With the following choice:

$$\begin{pmatrix} x \\ y \end{pmatrix} = \begin{bmatrix} \alpha^{-1} & \beta^{-1} \\ \alpha^{-1}(1-\sqrt{2})(\sqrt{3}-\sqrt{2}) & \beta^{-1}(1+\sqrt{2})(\sqrt{3}+\sqrt{2}) \end{bmatrix} \begin{pmatrix} X \\ Y \end{pmatrix}$$

where $\alpha = \sqrt{16-6\sqrt{6}-10\sqrt{2}+8\sqrt{3}}$ and $\beta = \sqrt{16+6\sqrt{6}+10\sqrt{2}+8\sqrt{3}}$,
the equations (9) and (10) read

$$\begin{aligned} \dot{X} &= \left(\lambda + 2a(X^2+Y^2) + 4b\left[(1+\sqrt{3})X^2 + (\sqrt{3}-3)Y^2\right]\right) X \\ \dot{Y} &= \left(\lambda + 2a(X^2+Y^2) + 4b\left[(1+\sqrt{3})Y^2 + (\sqrt{3}-3)X^2\right]\right) Y \end{aligned}$$

and $Q(X,Y) = 16bXY(X-Y)(X+Y)$. The axes $Y=0$ and $X=0$ correspond to $\widetilde{C}_{2\kappa}$ isotropy type and the axes $X = \pm Y$ correspond to $\widetilde{C}'_{2\kappa}$ isotropy type. Therefore if $b \neq 0$ there are no submaximal solutions in Fix(κ).

Stability of the solutions. The leading order of radial and transverse eigenvalues are computed from these equations and are summarized in Table 6.

Isotropy type	radial eigenvalue	transverse eigenvalue
$\widetilde{C}_{2\kappa}$	$4\left(a+2b(1+\sqrt{3})\right)X^2$	$-16bX^2$
$\widetilde{C}'_{2\kappa}$	$8\left(a+2b(\sqrt{3}-1)\right)X^2$	$32bX^2$

Table 6: Radial and transverse eigenvalues (leading order) of bifurcated branches in Fix(κ).

To summarize, under the condition that $a+2b(1+\sqrt{3}) < 0$ and $a+2b(\sqrt{3}-1) < 0$ (supercritical bifurcations), the bifurcation diagram in Fix(κ) is like in Figure 8 (upper left).

2. *Bifurcation and stability in* Fix(ϵ). By Lemma 7,

$$\mathrm{Fix}(\epsilon) = \{z_2 = (1+\mathbf{i})z_1 + \sqrt{3}\bar{z}_1\}.$$

By Table 5 there exist two axes of isotropy type $\widetilde{C}_{3\kappa'}$ and two of isotropy type $\widetilde{D}_3$.
We set $z_1 = x + \mathbf{i}y$. In (x,y) coordinates, $\mathrm{Fix}(\widetilde{C}_{3\kappa'}) = \{y = (1+\sqrt{2})x\}$ and $\mathrm{Fix}(\widetilde{D}_3) = \{(1+\sqrt{6}+2\sqrt{3})y = (2\sqrt{2}-3)x\}$.

We change coordinates so that $\mathrm{Fix}(\widetilde{C}_{3\kappa'})$ be the axis $Y=0$. With the following choice for the new coordinates:

$$\begin{pmatrix} x \\ y \end{pmatrix} = \begin{bmatrix} \alpha^{-1} & \beta^{-1}(\sqrt{3}+\sqrt{2}) \\ \alpha^{-1}(1+\sqrt{2}) & \beta^{-1}(1-\sqrt{2})(\sqrt{3}+\sqrt{2}) \end{bmatrix} \begin{pmatrix} X \\ Y \end{pmatrix}$$

where $\alpha = \sqrt{4+2\sqrt{2}}$ and $\beta = \sqrt{4-2\sqrt{2}}$, the equations in Fix($\epsilon$) have the simple form

$$\begin{aligned} \dot{X} &= \left(\lambda + 2a(3-\sqrt{6})(X^2+Y^2) + 4(\sqrt{3}-\sqrt{2})b(5X^2-3Y^2)\right) X \\ \dot{Y} &= \left(\lambda + 2a(3-\sqrt{6})(X^2+Y^2) + 4(\sqrt{3}-\sqrt{2})b((5Y^2-3X^2)\right) Y \ . \end{aligned}$$

Then $Q(X,Y) = 32b(\sqrt{3}-\sqrt{2})(X-Y)(X+Y)XY$, so we can conclude that if $b \neq 0$ no submaximal solution bifurcates in this plane.

Stability of the solutions. The leading orders of bifurcated branches and transverse eigenvalues are summarized in Table 7.

Isotropy type	radial eigenvalue	transverse eigenvalue
$\widetilde{C}_{3\kappa'}$	$8(\sqrt{3}-\sqrt{2})\left(a\sqrt{3}+10b\right)X^2$	$-32b(\sqrt{3}-\sqrt{2})X^2$
$\widetilde{D}_3$	$4(\sqrt{3}-\sqrt{2})\left(a\sqrt{3}+2b\right)X^2$	$64b(\sqrt{3}-\sqrt{2})X^2$

Table 7: Radial and transverse eigenvalues (leading order) of bifurcated equilibria in Fix(ϵ).

Therefore if $a\sqrt{3}+2b<0$ and $a\sqrt{3}+10b<0$, the stability diagram in Fix(ϵ) is like in Figure 8 (lower left).

3. *Bifurcation and stability in Fix(σ).* We consider instead Fix($\tilde{\sigma}$). By Lemma 7,

$$\mathrm{Fix}(\tilde{\sigma}) = \{(z_1,z_2)\in\mathbb{C}^2 | z_2 = (1-\sqrt{2})(\sqrt{2}z_1 + \mathbf{i}\sqrt{3}\bar{z}_1)\}$$

By Table 5 there are four axes of symmetry in this plane: one of type $\widetilde{C}_{2\kappa}$, one of type $\widetilde{C}'_{2\kappa}$, and two of type $\widetilde{D}_3$. We need to find a representative of $\widetilde{C}_{2\kappa}$ which contains $\tilde{\sigma} = \rho^2\sigma\rho^{-2}$. Since $\rho^2\kappa\rho^{-2} = -\kappa$ (easy check), this representative is $\widehat{C}_{2\kappa} = \langle\tilde{\sigma}, -\kappa\rangle$.
Let us write $x+\mathbf{i}y = z_1$. In the (x,y) coordinates, $\mathrm{Fix}(\widetilde{C}'_{2\kappa}) = \{x=y\}$ and $\mathrm{Fix}(\widehat{C}_{2\kappa}) = \{y=-x\}$. We change coordinates so that $Y = \frac{1}{\sqrt{2}}(x-y)$ and $X = \frac{1}{\sqrt{2}}(x+y)$. Hence $Y=0$ is the equation of $\mathrm{Fix}(\widetilde{C}'_{2\kappa})$ and $X=0$ is the equation of $\mathrm{Fix}(\widehat{C}_{2\kappa})$. Then

$$\begin{aligned}\dot{X} &= \left[\lambda + 2aC_1\left(X^2 - C_2Y^2\right) + 8bC_3X^2\right]X\\ \dot{Y} &= \left[\lambda + 2aC_1\left(X^2 - C_2Y^2\right) + 8bC_4Y^2\right]Y\end{aligned}$$

with the constants:

$$C_1 = 8+3\sqrt{6}-4\sqrt{3}-5\sqrt{2}>0 \quad C_2 = -10+4\sqrt{6}-5\sqrt{3}+6\sqrt{2}<0$$

$$C_3 = -10-4\sqrt{6}+6\sqrt{3}+7\sqrt{2}>0 \quad C_4 = 10-4\sqrt{6}+6\sqrt{3}-7\sqrt{2}>0$$

For this system we obtain

$$Q(X,Y) = -8bC_3(-X+C_5Y)(X+C_5Y)XY = 0$$

with $C_5 = (2+\sqrt{3})(\sqrt{2}-\sqrt{3}) < 0$.
The axes $X \pm C_5Y = 0$ correspond to the two copies of $\mathrm{Fix}(\widetilde{D}_3)$. By the same argument as before, this shows that no submaximal solution can bifurcate in Fix(σ) if $b\neq 0$.

Stability of the solutions. We proceed as in Fix(κ).
Radial eigenvalues have already been computed, see Tables 6 and 7. The leading order of transverse eigenvalues are summarized in Table 8.

Isotropy type	transverse eigenvalue
$\widetilde{C}_{2\kappa}$	$-8C_4bY^2$
$\widetilde{C}'_{2\kappa}$	$-8C_3bX^2$
$\widetilde{D}_3$	$16C_4bY^2$

Table 8: Transverse eigenvalues of bifurcated equilibria in Fix(σ).

It follows that if $a+2b(1+\sqrt{3})<0$, $a+2b(\sqrt{3}-1)<0$ and $a\sqrt{3}+2b<0$, the dynamics in Fix(σ) looks like the diagram in Figure 8 (upper right).

4. *Bifurcation and stability in* $\mathrm{Fix}(\kappa')$. We consider instead $\mathrm{Fix}(\kappa'')$. By Lemma 7,

$$\mathrm{Fix}(\kappa'') = \{(z_1, \bar{z}_1, z_2, \bar{z}_2) \mid z_2 = (\sqrt{3}-\sqrt{2})(-\sqrt{2}z_1 + \mathbf{i}\bar{z}_1)\}.$$

By Table 5 there are four axes of symmetry in this plane: one of type $\widetilde{C}_{2\kappa}$, one of type $\widetilde{C}'_{2\kappa}$, and two of type $\widetilde{C}_{3\kappa'}$. A direct computation with Maple shows that from Definition 2 a conjugate of $\widetilde{C}'_{2\kappa}$ containing κ'' is $\widehat{C}'_{2\kappa} = g\widetilde{C}'_{2\kappa}g^{-1} = \{Id, -\kappa, -\sigma, \kappa''\}$, with $g = \rho^3\hat{\sigma}\kappa$. Setting $z_1 = x + \mathbf{i}y$, the equations for $\mathrm{Fix}(\widetilde{C}_{2\kappa})$ and $\mathrm{Fix}(\widehat{C}'_{2\kappa})$ are respectively $x = y$ and $x = -y$. We do the change of coordinates $x = \sqrt{2}/2(X+Y)$, $x = \sqrt{2}/2(X-Y)$. The equations in these coordinates are

$$\begin{aligned}\dot{X} &= \left[\lambda + 2aD_1\left(-X^2 - D_2Y^2\right) + 8bD_3(-X^2 + D_4Y^2)\right]X \\ \dot{Y} &= \left[\lambda + 2aD_1\left(-X^2 - D_2Y^2\right) + \frac{4}{3}bD_5(-6X^2 + D_4)Y^2\right]Y\end{aligned}$$

where $D_1 = -8+3\sqrt{6}-4\sqrt{3}+5\sqrt{2}$, $D_2 = -6+2\sqrt{6}+3\sqrt{3}-4\sqrt{2}$, $D_3 = -10+4\sqrt{6}-6\sqrt{3}+7\sqrt{2}$, $D_4 = -27+10\sqrt{6}+15\sqrt{3}-18\sqrt{2}$ and $D_5 = -12+5\sqrt{6}-8\sqrt{3}+9\sqrt{2}$. Then $Q(X,Y) = 8b(-2+\sqrt{6}-2\sqrt{3}+2\sqrt{2})(X+(1+\sqrt{2})Y)(X-(1+\sqrt{2})Y)XY$, so we can again conclude that if $b \neq 0$ no submaximal solution bifurcates in this plane. The lines $X + (1 \pm \sqrt{2})Y$ correspond to the two axes with isotropy type $\widetilde{C}_{3\kappa'}$.

Stability of the solutions. Radial eigenvalues have already been computed, see Tables 6 and 7. The leading order of transverse eigenvalues are summarized in Table 9. If $a + 2b(1+\sqrt{3}) < 0$,

Isotropy type	transverse eigenvalue
$\widetilde{C}_{2\kappa}$	$8(2-\sqrt{6}+2\sqrt{3}-2\sqrt{2})bX^2$
$\widetilde{C}'_{2\kappa}$	$-8(2-\sqrt{6}-2\sqrt{3}+2\sqrt{2})bY^2$
$\widetilde{C}_{3\kappa'}$	$\dfrac{32bY^2}{2+\sqrt{6}-2\sqrt{3}-2\sqrt{2}}$

Table 9: Transverse eigenvalues of bifurcated equilibria in $\mathrm{Fix}(\sigma)$.

$a + 2b(\sqrt{3}-1) < 0$ and $a\sqrt{3} + 10b < 0$, the stability diagram in $\mathrm{Fix}(\epsilon)$ is like in Figure 8 (lower right).

2. Stability in $\mathbb{R}^4$. Observe first that equilibria with isotropies $\widetilde{C}_{2\kappa}$ and $\widetilde{C}'_{2\kappa}$ are never stable. Indeed their transverse eiganvalues in the planes $\mathrm{Fix}(\sigma)$ and $\mathrm{Fix}(\kappa')$ have opposite signs (we assume the generic condition $b \neq 0$ to be true). Now suppose that the solutions with isotropy $\widetilde{D}_3$ are supercritical, a condition which is fulfilled if $a\sqrt{3} + 2b < 0$. Their transverse eigenvalues in the invariant planes $\mathrm{Fix}(\epsilon)$ and $\mathrm{Fix}(\sigma)$ have the same sign as b. Moreover, the eigenvalue in $\mathrm{Fix}(\sigma)$ has multiplicity 2 in $\mathbb{R}^4$. Indeed the order 3 group element ϵ, acts by rotating this plane by an angle $2\pi/3$ around the axis $\mathrm{Fix}(\widetilde{D}_3)$. It follows that all non radial eigenvalues in $\mathbb{R}^4$ have the sign of b. If the bifurcation is supercritical and $b < 0$, these solutions are stable.
The same argument applies to solutions with isotropy $\widetilde{C}_{3\kappa'}$: transverse eigenvalues in the invariant planes $\mathrm{Fix}(\epsilon)$ and $\mathrm{Fix}(\kappa')$ have a sign opposite to the sign of b. The transverse eigenvalue in $\mathrm{Fix}(\kappa')$ is double in $\mathbb{R}^4$ by the same argument as before. It follows that if $a\sqrt{3}+10b < 0$ (supercritical branch) and $b > 0$, these solutions are stable in $\mathbb{R}^4$.
It remains to check the domain $\mathcal{P}$ in the theorem. One can easily check that all bifurcated branches are supercritical if the inequalities $a\sqrt{3}+2b < 0$ and $a\sqrt{3}+10b < 0$ are satisfied. This finishes the proof. □

4 Bifurcation diagrams in the case of the representation χ_{11}

4.1 Equivariant structure of the equations on the center manifold

As for representation χ_{12}, we also need to know the form of the asymptotic expansion of $f(\cdot, \lambda)$ in Equation (5). Table 15 of appendix B, given by the computation of Molien series, shows that there are

only one equivariant homogeneous polynomial map of order 3 and four linearily independant equivariant maps of order 5. The bifurcation diagrams are fully determined, under generic conditions, by the computations of these terms. However, it turns out that these computations are not anymore sufficient if one wants to study some specific dynamics of Equation (5) as depicted in section 5.

We first need to choose a system of coordinates in $\mathbb{R}^4$. The following lemma is proved in Appendix C.2.

Lemma 8. *For the representation χ_{11} the diagonalization of the 8-fold symmetry matrix ρ has the form*

$$\rho = \begin{bmatrix} \exp(\frac{\mathbf{i}\pi}{4}) & 0 & 0 & 0 \\ 0 & \exp(-\frac{\mathbf{i}\pi}{4}) & 0 & 0 \\ 0 & 0 & \exp(\frac{3\mathbf{i}\pi}{4}) & 0 \\ 0 & 0 & 0 & \exp(-\frac{3\mathbf{i}\pi}{4}) \end{bmatrix}$$

We note $(z_1, \bar{z}_1, z_2, \bar{z}_2)$ the complex coordinates in the corresponding basis.

Remark 3. *The diagonal matrix is the same as in Lemma 5, however the corresponding bases differ for the two representations χ_{12}, χ_{11}. Indeed, from Propositions 2 and 3 of Appendix A, one can check that the presentation given by biquaternions of ρ for representation χ_{12} and χ_{11} are different.*

The bifurcation equations of the center manifold is given by the following theorem.

Theorem 4. *For the representation χ_{11}, Equation (5) expressed in the coordinates $(z_1, \bar{z}_1, z_2, \bar{z}_2)$ admits the following expansion*

$$\begin{aligned} \dot{z}_1 = \lambda z_1 + A z_1 \left(|z_1|^2 + |z_2|^2\right) + a z_1 \left(|z_1|^2 + |z_2|^2\right)^2 + b\left(z_1^4 \bar{z}_2 + 4 z_2^3 |z_1|^2 - z_2^3 |z_2|^2\right) \\ + c\left(3\bar{z}_1^2 z_2 |z_2|^2 - z_1^2 \bar{z}_2^3 - 2\bar{z}_1^2 |z_1|^2 z_2\right) + d\left(-5\bar{z}_1^4 \bar{z}_2 + \bar{z}_2^5\right) + h.o.t \end{aligned} \quad (12)$$

$$\begin{aligned} \dot{z}_2 = \lambda z_2 + A z_2 \left(|z_1|^2 + |z_2|^2\right) + a z_2 \left(|z_1|^2 + |z_2|^2\right)^2 + b\left(-\bar{z}_1 z_2^4 - 4 z_1^3 |z_2|^2 + z_1^3 |z_1|^2\right) \\ + c\left(-3 z_1 \bar{z}_2^2 |z_1|^2 + \bar{z}_1^3 z_2^2 + 2 z_1 \bar{z}_2^2 |z_2|^2\right) + d\left(5\bar{z}_1 \bar{z}_2^4 - \bar{z}_1^5\right) + h.o.t \end{aligned} \quad (13)$$

where $(A, a, b, c, d) \in \mathbb{R}^5$.

Proof. There is one $\mathcal{G}$-equivariant cubic map, hence necessarily equals to $E_3(\mathbf{z}) = \mathbf{z}\|\mathbf{z}\|^2$ with $\mathbf{z} = (z_1, \bar{z}_1, z_2, \bar{z}_2)$. We postpone to Appendix C.2 the computation of the four quintic equivariant maps. □

4.2 Isotropy types and fixed points subspaces

Lemma 9. *The lattice of isotropy types for the representation χ_{11} is shown in Figure 9. The numbers in parentheses indicate the dimension of corresponding fixed-point subspaces.*

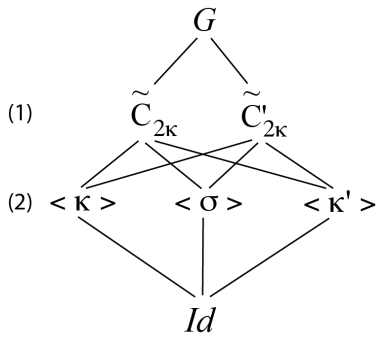

Figure 9: The lattice of isotropy types for the representation χ_{11}.

Proof. The only cyclic subgroups of $\mathcal{G}$ with a fixed-point subspace of positive dimension are given in the diagram of Figure 9 and determined by applying (8) for χ_{11} (see Table 3). The isotropy types with one-dimensional fixed-point subspace have been determined in [15], see Proposition 1. □

The next lemma gives expressions for the fixed-point subspaces of two-element groups in the $(z_1, \bar{z}_1, z_2, \bar{z}_2)$ coordinates, which will be usefull for the bifurcation analysis of (5) in the planes of symmetry. There are three types of these planes. We also express the fixed-point plane for the conjugate κ'' of κ' for later convenience.

Lemma 10. *Fixed-point subspaces associated with the isotropy groups in the diagram 9 have the following equations.*

- $Fix(\sigma) = \{(z_1, \bar{z}_1, z_2, \bar{z}_2) \mid z_2 = \mathbf{i}(1+\sqrt{2})z_1\}$;
- $Fix(\kappa) = \{(z_1, \bar{z}_1, z_2, \bar{z}_2) \mid z_1 = \mathbf{i}\bar{z}_1 \text{ and } z_2 = -\mathbf{i}\bar{z}_2\}$;
- $Fix(\kappa') = \{(z_1, \bar{z}_1, z_2, \bar{z}_2) \mid z_1 = \frac{\sqrt{2}}{2}(\mathbf{i}-1)\bar{z}_1 \text{ and } z_2 = \frac{\sqrt{2}}{2}(\mathbf{i}+1)\bar{z}_2\}$;
- $Fix(\kappa'') = \{(z_1, \bar{z}_1, z_2, \bar{z}_2) \mid z_2 = \mathbf{i}z_1 - \sqrt{2}\bar{z}_1\}$.

Proof. Given in Appendix D.2. □

The one dimensional fixed point subspaces are the intersections of planes of symmetry. This allows to easily obtain expressions for these axes from the expressions listed in Lemma 10. For example we can write

$$\mathrm{Fix}(\widetilde{C}_{2\kappa}) = \{(z_1, z_2) \in \mathbb{C}^2 \mid z_1 = \mathbf{i}\bar{z}_1 \text{ and } z_2 = \mathbf{i}(1+\sqrt{2})z_1\}.$$

4.3 Bifurcation analysis

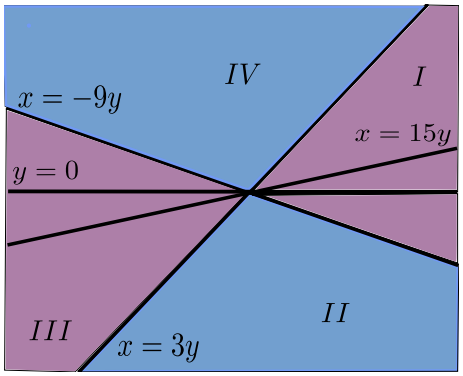

(a) In fixed-point plane $\mathrm{Fix}(\sigma)$, bifurcation of submaximal solutions occur for parameters (b, c, d) in the blue regions II and IV. We have set $x = b + c$ and $y = d$.

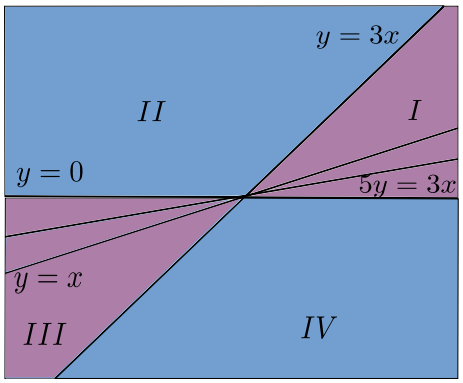

(b) In fixed-point plane $\mathrm{Fix}(\kappa'')$, bifurcation of submaximal solutions occur for parameters (b, c, d) in the blue regions II and IV. We have set $x = c$ and $y = b + d$.

Figure 10: Domain of existence of submaximal solutions in blue in the fixed-point planes $\mathrm{Fix}(\sigma)$ and $\mathrm{Fix}(\kappa'')$.

Theorem 5. *Provided that $A < 0$, there exists an attracting, flow invariant, sphere homeomorphic to S^3 in $\mathbb{R}^4$ and branches of equilibria with maximal isotropy (as listed in Proposition 1) are pitchfork and supercritical. The bifurcation diagrams in each fixed-point planes are as follows:*

(i) Fixed-point plane $Fix(\kappa)$.

- *No solution with submaximal isotropy bifurcates in fixed-point plane $Fix(\kappa)$.*
- *If $b < d$ (resp. $b > d$) the equilibria with isotropy $\widetilde{C}_{2\kappa}$ are stable (resp. saddles) and $\widetilde{C}'_{2\kappa}$ are saddles (resp. stable).*

This is summerized in Figure 11 in the case $b > d$.

(ii) Fixed-point plane Fix(σ).

- *If $b+c+9d > 0$ (resp. $b+c+9d < 0$) equilibria with isotropy $\widetilde{C}_{2\kappa}$ are stable (resp. saddles) and $\widetilde{C}'_{2\kappa}$ are saddles (resp. stable), regions I and IV (resp. II and III) in Figure 10(a).*
- *If $d(3d-b-c) < 0$ or $(b+c-15d)(b+c+9d) > 0$, no solution with submaximal isotropy bifurcates in fixed-point plane Fix(σ), regions I and III in Figure 10(a).*
- *If $d(3d-b-c) > 0$ and $(b+c-15d)(b+c+9d) < 0$, regions II and IV in Figure 10(a), solutions with submaximal isotropy bifurcate form equilibria $\widetilde{C}_{2\kappa}$ and $\widetilde{C}'_{2\kappa}$ in fixed-point plane Fix(σ). The corresponding bifurcation diagram is given in Figure 12.*

(iii) Fixed-point plane Fix(κ').

- *If $d+b-3c < 0$ (resp. $d+b-3c > 0$) equilibria with isotropy $\widetilde{C}_{2\kappa}$ are stable (resp. saddles) and $\widetilde{C}'_{2\kappa}$ are saddles (resp. stable), regions II and III (resp. I and IV) in Figure 10(b).*
- *If $(b+d)(b+d-c) < 0$ or $(5d-3c+5b)(d+b-3c) < 0$, no solution with submaximal isotropy bifurcates in fixed-point plane Fix(κ'), regions I and III in Figure 10(b).*
- *If $(b+d)(b+d-c) > 0$ or $(5d-3c+5b)(d+b-3c) > 0$, regions II and IV in Figure 10(b), solutions with submaximal isotropy bifurcate form equilibria $\widetilde{C}_{2\kappa}$ and $\widetilde{C}'_{2\kappa}$ in fixed-point plane Fix(κ'). The corresponding bifurcation diagram is given in Figure 12.*

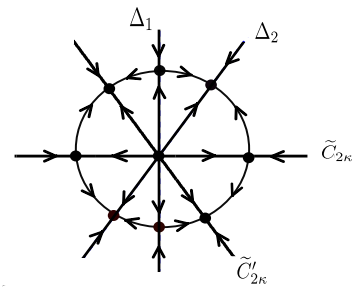

Figure 11: Bifurcation diagram in the plane Fix(κ) in the case $b > d$, see text. We denote Δ_1 (resp. Δ_2) the conjugate of $\widetilde{C}_{2\kappa}$ (resp. $\widetilde{C}'_{2\kappa}$) in Fix(κ).

Proof. The assumption $A < 0$ ensures that $\langle q(\xi), \xi\rangle = A\|\xi\|^4 < 0$ for all $\xi \neq 0$, where $\xi = (z_1, \bar{z}_1, z_2, \bar{z}_2)$, q is the cubic part in the equations (12), (13) and $\langle\ ,\ \rangle < 0$ denotes the inner product $\Re(z_1\bar{z}'_1 + z_2\bar{z}'_2)$ and $\|\ \|$ the associated norm. This implies the existence of the invariant sphere homeomorphic to S^3 in $\mathbb{R}^4$. We now examine bifurcation in the invariant planes. We can already note that, since $-Id$ acts non trivially in $\mathbb{R}^4 - \{0\}$ for χ_{12}, equilibria have to occur via pitchork bifurcations. The study in fixed-point planes for representation χ_{11} is exactly the same as the study for the irreductible representation χ_{12}.

1. *Bifurcation and stability in* Fix(κ). By Lemma 10,

$$\text{Fix}(\kappa) = \{(z_1, z_2) \in \mathbb{C}^2 | z_1 = (1+\mathbf{i})x \text{ and } z_2 = (1-\mathbf{i})y, \quad (x,y) \in \mathbb{R}^2\}\ .$$

By Table 5 this plane contains two axes with isotropy type $\widetilde{C}_{2\kappa}$ and two axes with isotropy type $\widetilde{C}'_{2\kappa}$. We can choose as representative $\text{Fix}(\widetilde{C}_{2\kappa}) = \{y = -(1+\sqrt{2})x\}$ and $\text{Fix}(\widetilde{C}'_{2\kappa}) = \{y = (1+\sqrt{2})x\}$. We change coordinates so that $\text{Fix}(\widetilde{C}_{2\kappa})$ is the real axis. With the following choice:

$$\begin{pmatrix} x \\ y \end{pmatrix} = \begin{bmatrix} \alpha^{-1} & \beta^{-1} \\ -\alpha^{-1}(1+\sqrt{2}) & \beta^{-1}(\sqrt{2}-1) \end{bmatrix} \begin{pmatrix} X \\ Y \end{pmatrix}$$

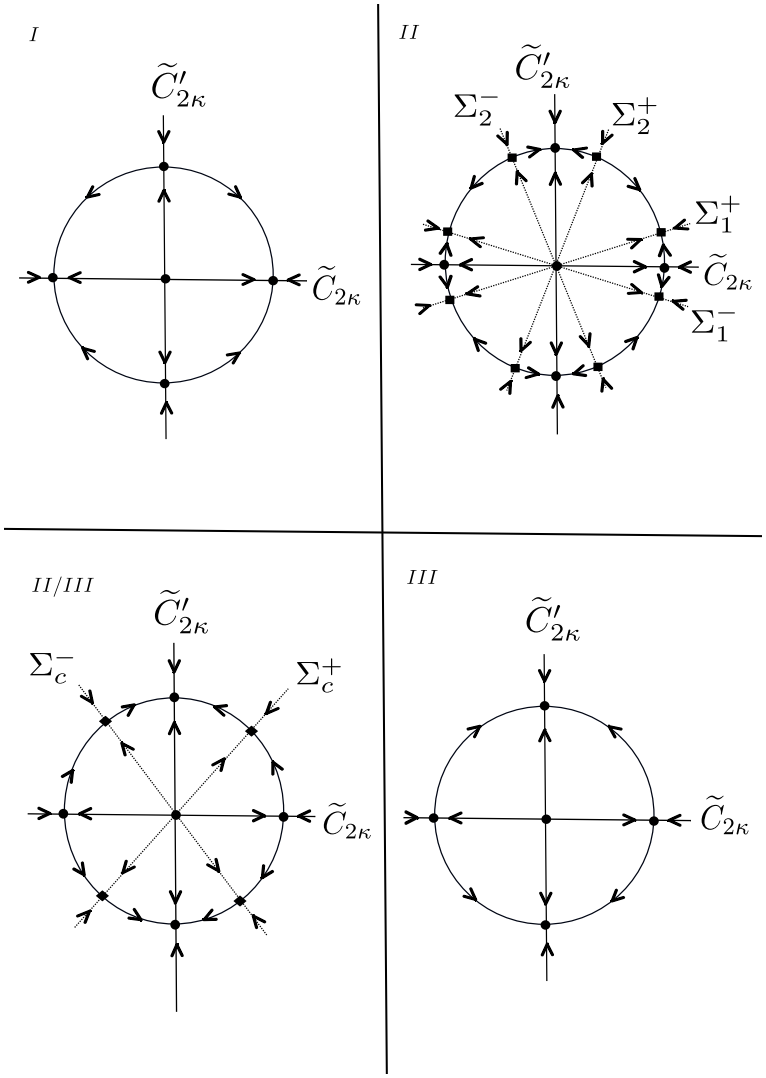

Figure 12: Generic bifurcation diagrams when parameters pass from regions $I - II - III$ in Figure 10(a) for fixed-point plane $\mathrm{Fix}(\sigma)$ and Figure 10(b) for fixed-point plane $\mathrm{Fix}(\kappa')$. • $I \to II$. Pitchfork bifurcation with submaximal isotropy occurs and two equilibria $\Sigma_1^{\pm}$ emerge from equilibria with isotropy type $\widetilde{C}_{2\kappa}$ and two equilibria $\Sigma_2^{\pm}$ emerge from equilibria with isotropy type $\widetilde{C}'_{2\kappa}$ with exchange of stability: $\widetilde{C}_{2\kappa}$ becomes unstable and $\widetilde{C}'_{2\kappa}$ stable, which implies that $\Sigma_1^{\pm}$ are stable and $\Sigma_2^{\pm}$ are saddles (upper right). • $II - III$ At the boundary between region II and III, equilibria Σ_1^+ (resp. Σ_1^-) and Σ_2^+ (resp. Σ_2^-) collide and form only one equilibrium denoted Σ_c^+ (resp. Σ_c^-), which no longer exists in region III: fold bifurcation. These two equilibria $\Sigma_c^{\pm}$ are saddles. • III, equilibria with isotropy type $\widetilde{C}_{2\kappa}$ are now unstable whereas equilibria with isotropy type $\widetilde{C}'_{2\kappa}$ are stable.

where $\alpha = \sqrt{4+2\sqrt{2}}$ and $\beta = \sqrt{4-2\sqrt{2}}$, the equations (12) and (13) read

$$\dot{X} = \lambda X + 2AX(X^2+Y^2) + 4aX(X^2+Y^2)^2 + 2bX(-X^4 - 2X^2Y^2 + 7Y^4) \\ + 2cX(X^4 - 6X^2Y^2 + Y^4) + 2dX(3X^4 - 10X^2Y^2 - 5Y^4)$$

$$\dot{Y} = \lambda Y + 2AY(X^2+Y^2) + 4aY(X^2+Y^2)^2 - 2bY(-7X^4 + 2X^2Y^2 + Y^4) \\ + 2cY(X^4 - 6X^2Y^2 + Y^4) - 2dY(5X^4 + 10X^2Y^2 - 3Y^4)$$

and the polynomial map Q defined in Equation (11) is $Q(X,Y) = -16(X-Y)(X+Y)(X^2+Y^2)XY(b-d)$. The axes $Y=0$ and $X=0$ correspond to $\widetilde{C}_{2\kappa}$ isotropy type and the axes $X=\pm Y$ correspond to $\widetilde{C}'_{2\kappa}$ isotropy type. Therefore if $b \neq d$ there are no submaximal solutions in $\mathrm{Fix}(\kappa)$.

Stability of the solutions. The leading order of radial and transverse eigenvalues are computed from these equations and are summarized in Table 10.

Isotropy type	radial eigenvalue	transverse eigenvalue
$\widetilde{C}_{2\kappa}$	$4AX^2$	$16(b-d)X^4$
$\widetilde{C}'_{2\kappa}$	$8AX^2$	$-64(b-d)X^4$

Table 10: Radial and transverse eigenvalues (leading order) of bifurcated branches in $\mathrm{Fix}(\kappa)$.

To summarize, under the condition that $A<0$ (supercritical bifurcations), the bifurcation diagram in $\mathrm{Fix}(\kappa)$ is like in Figure 11.

2. *Bifurcation and stability in* $\mathrm{Fix}(\sigma)$. By Lemma 10,

$$\mathrm{Fix}(\sigma) = \{(z_1,z_2) \in \mathbb{C}^2 \mid z_2 = \mathbf{i}(1+\sqrt{2})z_1\} .$$

By Table 5 there are two axes of symmetry in this plane: one of type $\widetilde{C}_{2\kappa}$ and one of type $\widetilde{C}'_{2\kappa}$. From Definition 2, a conjugate of $\widetilde{C}'_{2\kappa}$ containing σ is $\widetilde{C}''_{2\kappa} = \rho^{-2}\widetilde{C}'_{2\kappa}\rho^2 = \{Id, \sigma, -\kappa, -\kappa''\}$.

Let us write $z_1 = x + \mathbf{i}y$. In the (x,y) coordinates, $\mathrm{Fix}(\widetilde{C}_{2\kappa}) = \{y=x\}$, $\mathrm{Fix}(\widetilde{C}''_{2\kappa}) = \{y=-x\}$. We change coordinates such that $x = \sqrt{2}/2(X+Y)$, $x = \sqrt{2}/2(X-Y)$. Hence $Y=0$ is the equation of $\mathrm{Fix}(\widetilde{C}_{2\kappa})$ and $X=0$ is the equation of $\mathrm{Fix}(\widetilde{C}''_{2\kappa})$. Then

$$\dot{X} = \lambda X + 2E_1AX(X^2+Y^2) + 8E_2aX(X^2+Y^2)^2 - 4E_2bX(X^2+Y^2)(X^2-3Y^2) \\ + 4E_2cX(X^2+Y^2)^2 + 12E_2dX(X^4 - 10X^2Y^2 + 5Y^4)$$

$$\dot{Y} = \lambda Y + 2E_1AY(X^2+Y^2) + 8E_2aY(X^2+Y^2)^2 - 4E_2bY(X^2+Y^2)(3X^2-Y^2) \\ - 4E_2cY(X^2+Y^2)^2 - 12E_2dX(5X^4 - 10X^2Y^2 + Y^4)$$

where $E_1 = 2+\sqrt{2}$ and $E_2 = 3+2\sqrt{2}$. For this system we obtain

$$Q(X,Y) = 8E_2XY\left[(b+c+9d)X^4 + 2(b+c-15d)X^2Y^2 + (b+c+9d)Y^4\right]$$

We denote $H(X,Y) = (b+c+9d)X^4 + 2(b+c-15d)X^2Y^2 + (b+c+9d)Y^4$.

Study of the polynomial map $H(X,Y)$. We consider H as a polynomial map of degree two in X^2. When $b+c-15d=0$, then H is simplified as $H(X,Y) = (b+c+9d)(X^4+Y^4)$, and there is no submaximal bifurcation in $\mathrm{Fix}(\sigma)$. In the remaining part of this paragraph, we suppose that $b+c-15d \neq 0$. The discriminant of H is given by $\delta = 192d(3d-b-c)Y^4$.

- Suppose that $d(3d-b-c)>0$ then $X^2=\nu_\pm Y^2$ with

$$\nu_\pm=\frac{-(b+c-15d)\pm\sqrt{48d(3d-b-c)}}{(b+c+9d)}$$

with $\nu_+\nu_-=1$ and $\nu_++\nu_-=-2\frac{b+c-15d}{b+c+9d}$. We deduce that if $\frac{b+c-15d}{b+c+9d}<0$, there are four axes $X=\pm\sqrt{\nu_\pm}Y$ which correspond to bifurcated submaximal solutions in $\mathrm{Fix}(\sigma)$. If $\frac{b+c-15d}{b+c+9d}>0$ no submaximal bifurcation can bifurcate in $\mathrm{Fix}(\sigma)$.
- Suppose that $d=0$ and $b+c\neq 0$ then $H(X,Y)=(b+c)(X^2+Y^2)^2$. This implies that no submaximal bifurcation can bifurcate in $\mathrm{Fix}(\sigma)$ if $d=0$ and $b+c\neq 0$.
- If $3d=b+c$ and $d\neq 0$ then $H(X,Y)=12d(X-Y)^2(X+Y)^2$ and the axes $X=\pm Y$ correspond to bifurcated submaximal solutions in $\mathrm{Fix}(\sigma)$.
- If we suppose that $d(3d-b-c)<0$ then H has no other root than $(0,0)$. By the same argument as before, this shows that no submaximal solution can bifurcate in $\mathrm{Fix}(\sigma)$ if $d(3d-b-c)<0$.

Stability of the solutions. The leading order of radial and transverse eigenvalues for isotropy type $\widetilde{C}_{2\kappa}$ and $\widetilde{C}'_{2\kappa}$ are computed from the above equations and are summarized in Table 11.

Isotropy type	radial eigenvalue	transverse eigenvalue
$\widetilde{C}_{2\kappa}$	$4(2+\sqrt{2})AX^2$	$-8(3+2\sqrt{2})(b+c+9d)X^4$
$\widetilde{C}'_{2\kappa}$	$4(2+\sqrt{2})AX^2$	$8(3+2\sqrt{2})(b+c+9d)X^4$

Table 11: Radial and transverse eigenvalues (leading order) of bifurcated branches in $\mathrm{Fix}(\sigma)$.

We know discuss the stability of the bifurcated submaximal solutions found for $d(3d-b-c)>0$ and $(b+c-15d)(b+c+9d)<0$, i.e regions II and IV of Figure 10(a). We denote Σ_1^+ (resp. Σ_1^-) the branch of solutions with axis $X=\sqrt{\nu_+}Y$ (resp. $X=-\sqrt{\nu_+}Y$) and Σ_2^+ (resp. Σ_2^-) the branch of solutions with axis $X=\sqrt{\nu_-}Y$ (resp. $X=-\sqrt{\nu_-}Y$). When parameters pass from region I to region II in Figure 10(a), pitchfork bifurcation with submaximal isotropy occurs and two equilibria $\Sigma_1^\pm$ emerge from equilibria with isotropy type $\widetilde{C}_{2\kappa}$ and two equilibria $\Sigma_2^\pm$ emerge from equilibria with isotropy type $\widetilde{C}'_{2\kappa}$ with exchange of stability: $\widetilde{C}_{2\kappa}$ becomes unstable and $\widetilde{C}'_{2\kappa}$ stable, which implies that $\Sigma_1^\pm$ are stable and $\Sigma_2^\pm$ are saddles, see Figure 12 (upper right). At the boundary between region II and III, equilibria Σ_1^+ (resp. Σ_1^-) and Σ_2^+ (resp. Σ_2^-) collide and form only one equilibrium denoted Σ_c^+ (resp. Σ_c^-), which no longer exists in region III: saddle-node bifurcation. These two equilibria $\Sigma_c^\pm$ are saddles, see Figure 12 (lower left). In region III, equilibria with isotropy type $\widetilde{C}_{2\kappa}$ are now unstable whereas equilibria with isotropy type $\widetilde{C}'_{2\kappa}$ are stable, see Figure 12 (lower right). Same phenomena occur when values of the parameters pass from region III to region I through region IV in figure 10(a). We summerize the positive section of the bifurcation diagrams of Figure 12 in Figure 13.

3. *Bifurcation and stability in* $\mathrm{Fix}(\kappa')$. We consider instead $\mathrm{Fix}(\kappa'')$. By Lemma 10,

$$\mathrm{Fix}(\kappa'')=\{(z_1,\bar{z}_1,z_2,\bar{z}_2)\mid z_2=\mathbf{i}z_1-\sqrt{2}\bar{z}_1\}\ .$$

By Table 5 there are two axes of symmetry in this plane: one of type $\widetilde{C}_{2\kappa}$ and one of type $\widetilde{C}'_{2\kappa}$. We have already noticed that a conjugate of $\widetilde{C}'_{2\kappa}$ which contains κ'' is $\widehat{C}'_{2\kappa}=\{Id,-\sigma,-\kappa,\kappa''\}$. Setting $z_1=x+\mathbf{i}y$, the equations for $\mathrm{Fix}(\widetilde{C}_{2\kappa})$ and $\mathrm{Fix}(\widehat{C}'_{2\kappa})$ are respectively $y=x$ and $y=-x$. With the change of coordinates $x=\sqrt{2}/2(X+Y)$, $x=\sqrt{2}/2(X-Y)$ the equations become:

$$\begin{aligned}\dot{X}=\lambda X&+2E_1AX(X^2+E_3^2Y^2)+8E_2aX(X^2+E_3^2Y^2)^2\\&+4E_2bX(-X^2+2\sqrt{2}E_3XY+E_3^2Y^2)(X^2+2\sqrt{2}E_3XY-E_3^2Y^2)\\&+4E_2cX(X^2-5E_3^2Y^2)(X-E_3Y)(X+E_3Y)+4E_2dX(3X^4+10E_3^2X^2Y^2-5E_3^4Y^4)\end{aligned}$$

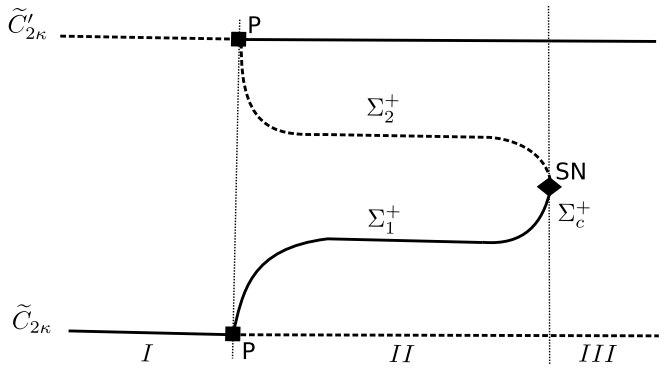

Figure 13: Positive section of the bifurcation diagrams of Figure 12 when parameters pass from regions $I-II-III$. Dashed lines represent unstable branches and continuous lines represent stable branches. ■-P stands for pitchfork bifurcation and ♦-SN for saddle-node bifurcation, see text for notations.

$$\begin{aligned}\dot{Y} = \lambda Y &+ 2E_1AY(X^2+E_3^2Y^2) + 8E_2aY(X^2+E_3^2Y^2)^2\\ &- 4E_2bY(-X^2+2\sqrt{2}E_3XY+E_3^2Y^2)(X^2+2\sqrt{2}E_3XY-E_3^2Y^2)\\ &- 4E_2cY(5X^2-E_3^2Y^2)(X-E_3Y)(X+E_3Y) + 4E_2dY(5X^4-10E_3^2X^2Y^2-3E_3^4Y^4)\end{aligned}$$

where $E_3 = 1-\sqrt{2}$. Then

$$Q(X,Y) = -8E_2XY\left[(b+d-3c)X^4 - 2E_3^2(5d+5b-3c)X^2Y^2 + E_3^4(b+d-3c)Y^4\right]$$

We denote $K(X,Y) = (b+d-3c)X^4 - 2E_3^2(5d+5b-3c)X^2Y^2 + E_3^4(b+d-3c)Y^4$.

Study of the polynomial map $K(X,Y)$. We consider K as a polynomial of degre two in X^2. If $5d+5b-3c=0$, then $K(X,Y) = (b+d-3c)(X^4+E_3^4Y^4)$, and no submaximal bifurcation can occur in fixed-point plane $\mathrm{Fix}(\kappa'')$. In the remaining part of this discussion, we suppose that $5d+5b-3c\neq 0$. The discriminant of $K(X,Y)$ is given by $\delta = 96E_3^4(b+d)(b+d-c)$.

- Suppose $(b+d)(b+d-c)>0$ then $X^2=\nu_\pm Y^2$ with

$$\nu_\pm = E_3^2\frac{5d-3c+5b\pm 2\sqrt{6(b+d)(b+d-c)}}{(d+b-3c)}Y^2$$

  where $\nu_+\nu_- = C^2$ and $\nu_+ + \nu_- = 2E_3^2\frac{5d-3c+5b}{d+b-3c}$. This implies that if $(5d-3c+5b)(d+b-3c)>0$ there are four axes $X=\pm\sqrt{\nu_\pm}Y$ which correspond to bifurcated submaximal solutions in $\mathrm{Fix}(\kappa'')$. And if $(5d-3c+5b)(d+b-3c)<0$, no submaximal solution can bifurcate in this plane.
- If $b+d=c$ and $c\neq 0$, then $K(X,Y) = -2c(X^2+E_3^2Y^2)^4$. There is no bifurcated submaximal solution in $\mathrm{Fix}(\kappa'')$.
- Suppose that $d+b=0$ and $c\neq 0$, then $K(X,Y) = -3c(X^2-E_3^2Y^2)^2$ and the axes $X=\pm E_3Y$ correspond to bifurcated submaximal solutions in $\mathrm{Fix}(\kappa'')$.
- Finally, if $(b+d)(b+d-c)<0$, then K has no other root than $(0,0)$. By the same argument as before, this shows that no submaximal solution can bifurcate in fixed-point plane $\mathrm{Fix}(\kappa'')$.

Stability of the solutions. The leading order of radial and transverse eigenvalues for isotropy type $\widetilde{C}_{2\kappa}$ and $\widetilde{C}'_{2\kappa}$ are computed from the above equations and are summarized in Table 12.

The bifurcation analysis of submaximal solutions is the same as in fixed-point plane $\mathrm{Fix}(\sigma)$ and presents no difficulty.

Isotropy type	radial eigenvalue	transverse eigenvalue
$\widetilde{C}_{2\kappa}$	$4(2+\sqrt{2})AX^2$	$8(3+2\sqrt{2})(d+b-3c)X^4$
$\widetilde{C}'_{2\kappa}$	$4(2-\sqrt{2})AX^2$	$-8(3-2\sqrt{2})(d+b-3c)X^4$

Table 12: Radial and transverse eigenvalues (leading order) of bifurcated branches in Fix(κ'').

□

Remark 4. *From Tables 10, 11 and 12, we deduce that there always exists a range of parameters such that equilibria with isotropy type $\widetilde{C}_{2\kappa}$ and $\widetilde{C}'_{2\kappa}$ are unstable. We also point out that, to leading order, the sign of transverse eigenvalues for isotropy type $\widetilde{C}_{2\kappa}$ is the opposite of the sign of transverse eigenvalues for isotropy type $\widetilde{C}'_{2\kappa}$.*

We can choose coordinates to express fixed-point lines Fix($\widetilde{C}_{2\kappa}$) and Fix($\widetilde{C}'_{2\kappa}$) in $\mathbb{R}^4$ as Fix($\widetilde{C}_{2\kappa}$) $= \{(x, x, -(1+\sqrt{2})x, (1+\sqrt{2})x) \mid x \in \mathbb{R}\}$ and Fix($\widetilde{C}'_{2\kappa}$) $= \{(x, -x, (1+\sqrt{2})x, (1+\sqrt{2})x) \mid x \in \mathbb{R}\}$. We summerize in Table 13, to leading order, radial and transverse eigenvalues (denoted t_k, $k = 1 \dots 3$) of bifurcated branches $\widetilde{C}_{2\kappa}$ and $\widetilde{C}'_{2\kappa}$ in $\mathbb{R}^4$.

Isotropy type	$\widetilde{C}_{2\kappa}$	$\widetilde{C}'_{2\kappa}$
Radial eigenvalue	$8(2+\sqrt{2})Ax^2$	$8(2+2\sqrt{2})Ax^2$
t_1	$128(3+2\sqrt{2})(b-d)x^4$	$-128(3+2\sqrt{2})(b-d)x^4$
t_2	$-32(3+2\sqrt{2})(b+c+9d)x^4$	$32(3+2\sqrt{2})(b+c+9d)x^4$
t_3	$32(3+2\sqrt{2})(b+d-3c)x^4$	$-32(3+2\sqrt{2})(b+d-3c)x^4$

Table 13: Radial and transverse eigenvalues (leading order) of bifurcated branches in $\mathbb{R}^4$.

5 Bifurcation of a heteroclinic network in the χ_{11} case

5.1 Existence

We suppose now that the cubic term coefficient $A < 0$, and by a suitable chage of time scale we can take $A = -1$. This implies, as shown in Theorem 5, that a flow-invariant S^3 sphere bifurcates for Equations (12) and (13). The system reads:

$$\begin{cases} \dot{z}_1 &= \lambda z_1 - z_1\left(|z_1|^2+|z_2|^2\right) + az_1\left(|z_1|^2+|z_2|^2\right)^2 + b\left(z_1^4\bar{z}_2 + 4z_2^3|z_1|^2 - z_2^3|z_2|^2\right) \\ &\quad +c\left(3\bar{z}_1^2 z_2|z_2|^2 - z_1^2\bar{z}_2^3 - 2\bar{z}_1^2|z_1|^2 z_2\right) + d\left(-5\bar{z}_1^4\bar{z}_2 + \bar{z}_2^5\right) + h.o.t. \\ \dot{z}_2 &= \lambda z_2 - z_2\left(|z_1|^2+|z_2|^2\right) + az_2\left(|z_1|^2+|z_2|^2\right)^2 + b\left(-\bar{z}_1 z_2^4 - 4z_1^3|z_2|^2 + z_1^3|z_1|^2\right) \\ &\quad +c\left(-3z_1\bar{z}_2^2|z_1|^2 + \bar{z}_1^3 z_2^2 + 2z_1\bar{z}_2^2|z_2|^2\right) + d\left(5\bar{z}_1\bar{z}_2^4 - \bar{z}_1^5\right) + h.o.t. \end{cases} \tag{14}$$

In the sequel we also suppose that coefficients (b, c, d) satisfy the following conditions:

- **C1**: $b - d > 0$
- **C2**: $d(3d - b - c) < 0$ and $b + c + 9d > 0$
- **C3**: $(b + d)(b + d - c) < 0$ and $b + d - 3c < 0$

Under these conditions all bifurcated equilibria have maximal isotropy and moreover, according to Remark 4, none of them is stable. More precisely, condition **C1** implies that saddle-sink heteroclinic orbits connect in the plane Fix(κ) equilbria of isotropy type $\widetilde{C}_{2\kappa}$ to equilibria with isotropy type $\widetilde{C}'_{2\kappa}$ (figure 11). Condition **C2** implies that saddle-sink heteroclinic orbits connect in the plane Fix(σ) equilibria with isotropy type $\widetilde{C}'_{2\kappa}$ to equilibria with isotropy type $\widetilde{C}_{2\kappa}$ (case I in figure 12). In the same fashion, saddle-sink heteroclinic orbits connect in the plane Fix(κ'') equilibria with isotropy type $\widetilde{C}_{2\kappa}$ to eqiulibria with isotropy type $\widetilde{C}'_{2\kappa}$ when condition **C3** is satisfied.

These heteroclinic orbits are robust against $\mathcal{G}$-equivariant perturbations. Their $\mathcal{G}$-orbit realizes a *heteroclinic network* between the $\mathcal{G}$-orbits of equilibria of types $\widetilde{C}_{2\kappa}$ and $\widetilde{C}'_{2\kappa}$.

Notice that under the above hypotheses the equilibria of type $\widetilde{C}_{2\kappa}$ have a one dimensional unstable manifold, while equilibria of type $\widetilde{C}'_{2\kappa}$ have a two dimensional unstable manifold which contains the heteroclinic orbits lying in the planes of type $\mathrm{Fix}(\sigma)$ and $\mathrm{Fix}(\kappa'')$.

The existence of a heteroclinic network can lead to interesting non trivial dynamics characterized by long periods of quasi-static state (trajectory approaches an equilibrium of the cycle) followed by a fast excursion far from equilibrium and relaxation to another quasi-static state, the process being repeated in an aperiodic way [12, 2, 23]. This point will be considered in Section 5.3, but we first simplify the problem by proceeding to a suitable orbit space reduction.

5.2 Quotient network

The heteroclinic network introduced above has 48 nodes (equilibria) and 144 edges (heteroclinic orbits). Indeed the isotropy subgroups $\widetilde{C}_{2\kappa}$ and $\widetilde{C}'_{2\kappa}$ have order 4, hence the orbits of equilibria with these isotropies have $|\mathcal{G}|/4 = 24$ elements each. To each node of type $\widetilde{C}_{2\kappa}$ are associated 2 "outgoing" edges and 4 "incoming" edges. There are 48 nodes but each edge has two ends, hence the result. We can simplify this structure by projecting the system onto the quotient space (orbit space) $S^3/\mathcal{G}$ where S^3 is the flow-invariant sphere. This procedure would project the network onto a simpler one in which there are only two nodes. Moreover the trajectories of the equivariant vector field in S^3 project on trajectories for a smooth vector field defined on the orbit space [12]. However this orbit space is not a manifold (it would be if the action of $\mathcal{G}$ were free) and its geometric, stratified structure is too difficult to compute to make this method useful in our case. We can however proceed as [1] by identifying a subgroup $\mathcal{G}_0$ of $\mathcal{G}$ with a free action on S^3 and large enough to allow for a substantial reduction of the number of equilibria on the 3-dimenisonal manifold $S^3/\mathcal{G}_0$. This is the aim of the next lemma.

Lemma 11. *The group $\mathcal{G}_0$ generated by the elements ρ^2 and ϵ has 24 elements. It acts fixed-point free on S^3 and the two $\mathcal{G}$-orbits of equilibria on S^3 reduce to a pair of equilibria in the manifold $S_3/\mathcal{G}_0$ for the projected dynamics.*

Proof. In Table 4 of [15], $\mathcal{G}_0$ is identified with the 24 element group $SL(2,3)$, the group of 2×2 matrices over the field $\mathbb{Z}_3$. Since none of its elements appears in the isotropy subgroups of $\mathcal{G}$ for the representation χ_{11}, its elements only fix the origin. For the same reason $\mathcal{G}_0$ acts fixed point free on the 24 elements orbits of equilibria and by taking the quotient by this action these orbits reduce to single equilibria. □

It follows that the heteroclinic network "drops down" to a quotient heteroclinic network between the two equilibria which we denote by A ($\widetilde{C}_{2\kappa}$ type) and B ($\widetilde{C}'_{2\kappa}$ type) in $S^3/\mathcal{G}_0$. There are two connections from A to B and four connections from B to A, as it can be seen in Figure 14. This projected heteroclinic network can be seen as the union of eight *heteroclinic cycles* which however belong to two symmetry classes only: the cycles $1\to 5$, $2\to 5$, $1\to 6$, $2\to 6$ are exchanged by reflection symmetries (projected on $S^3/\mathcal{G}_0$), same thing for the cycles $3\to 5$, $4\to 5$, $3\to 6$, $4\to 6$. We call ν-cycle (resp. μ-cycle) the cycle $1\to 5$ (resp. $4\to 5$). We denote ν_A, ν_B (resp. μ_A, μ_B) the eigenvalues at A and B along the connection $1-2$ (resp. $3-4$).

5.3 Asymptotic stability

The asymptotic stability of heteroclinic cycles has been studied by several authors [33, 34, 3, 35] and sufficient conditions on the ratio of eigenvalues "along" the cycle have been provided to ensure this property generically. Roughly speaking, the attractiviness property of a heteroclinic cycle is determined by the relative strength of the contracting and expanding eigenvalues along the cycle, computed at the equilibria in the cycle. If at an equilibrium in the cycle the unstable manifold has dimension >1 and does not realize a saddle-sink connection to other equilibria in some fixed-point subspace, the heteroclinic cycle can not be asymptotically stable in the usual sense, that is asymptotically attracting for initial conditions in an open tubular neighborhood of the cycle. As shown by Krupa and Melbourne in [34], it can still have a weaker attractiviness property which they called essential stability: under certain conditions on the eigenvalues the heteroclinic cycle is attracting for initial conditions belonging to the complement of a cuspidal region in a tubular neighborhood of the cycle.

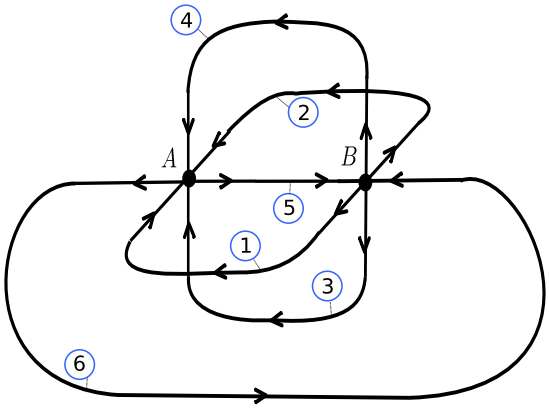

Figure 14: Representation of the quotient heteroclinic network between equilibria A ($\widetilde{C}_{2\kappa}$ type) and B ($\widetilde{C}'_{2\kappa}$ type) in $S^3/\mathcal{G}_0$. Heteroclinic connections denoted $1, 2$, which link B to A, result of the quotient in $S^3/\mathcal{G}_0$ of the heteroclinic connections which connect $\widetilde{C}''_{2\kappa}$ to $\widetilde{C}_{2\kappa}$ in $\mathrm{Fix}(\sigma)$. Heteroclinic connections denoted $3, 4$, which link B to A, result of the quotient in $S^3/\mathcal{G}_0$ of the heteroclinic connections which connect $\widehat{C}_{2\kappa}$ to $\widetilde{C}'_{2\kappa}$ in $\mathrm{Fix}(\kappa'')$. Heteroclinic connections denoted $5, 6$, which link A to B, result of the quotient in $S^3/\mathcal{G}_0$ of the heteroclinic connections which connect $\widetilde{C}_{2\kappa}$ to $\widetilde{C}'_{2\kappa}$ in $\mathrm{Fix}(\kappa)$.

A heteroclinic network is a union of cycles. As observed by Kirk and Silber [31] those cycles can not be simultaneously essentially stable but conditions can be derived to determine which one is. In this section we derive sufficient conditions for the essential stability of the two cycles in our heteroclinic network projected on the orbit space $S^3/\mathcal{G}_0$.

First we simplify notation by denoting $(\lambda_A, -\nu_A, -\mu_A)$ the eigenvalues at equilibrium A and $(-\lambda_B, \nu_B, \mu_B)$ the eigenvalues at equilibrium B. We consider:

$$\lambda_e > 0, \quad \nu_e > 0, \quad \mu_e > 0 \quad e = A, B$$

We cannot apply directly theorems of [33] but we will proceed in the same fashion as in [31]. In the following, we suppose without loss of generality that:

$$\nu_B > \mu_B \tag{15}$$

We define:

$$\rho_\mu = \frac{\mu_A \lambda_B}{\lambda_A \mu_B}, \quad \sigma_\mu = \frac{\mu_A}{\lambda_A}\left[\frac{\nu_B}{\mu_B} - \frac{\nu_A}{\mu_A}\right], \quad \rho_\nu = \frac{\nu_A \lambda_B}{\lambda_A \nu_B}, \quad \sigma_\nu = \frac{\nu_A}{\lambda_A}\left[\frac{\mu_B}{\nu_B} - \frac{\mu_A}{\nu_A}\right]$$

Theorem 6. *(i) Suppose that $\rho_\mu > 1$ and $\rho_\nu > 1$.*

1. *If $\sigma_\nu < 0$ and $\sigma_\mu > 0$, almost all orbits passing through a tubular neighborhood of the μ-cycle escape this neighborhood in finite time, exceptions being those orbits that lie in the stable manifolds of A or B. The ν-cycle is* essentially asymptotically stable*: it attracts almost all trajectories starting in a small enough tubular neighborhood of it, the only possible exceptions being those orbits that pass through a cuspoidal region abutting the heteroclinic connection from A to B.*

2. *If $\sigma_\nu > 0$ and $\sigma_\mu < 0$, almost all orbits passing through a tubular neighborhood of the ν-cycle escape this neighborhood in finite time, exceptions being those orbits that lie in the stable manifolds of A or B. The μ-cycle is* essentially asymptotically stable*: it attracts almost all trajectories starting in a small enough tubular neighborhood of it, the only possible exceptions being those orbits that pass through a cuspoidal region abutting the heteroclinic connection from A to B.*

(ii) Suppose that $0 < \rho_\mu < 1$ (resp. $0 < \rho_\nu < 1$). Then the μ-cycle (resp. ν-cycle) repels almost all orbits and the attractivity properties of the ν-cycle (esp. μ-cycle) are determined by σ_ν (resp. σ_μ) as above.

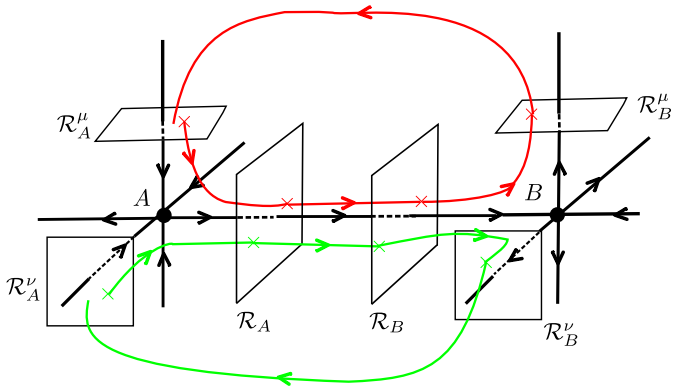

Figure 15: First return map in S^3.

Proof. We first linearize the flow in neighborhoods of A and B by a continous change of variables [26, 11]. We can further choose local coordinates such that the local stable and unstable manifold of A and B are either the horizontal axis or the vertical plane. Using Euclidean coordinates (v, w) in the vertical plane and u for the horizontal axis, we have for A:

$$W^u_{loc}(A) = \{(u, 0, 0) \mid u \in \mathbb{R}\} \quad W^s_{loc}(A) = \{(0, v, w) \mid (v, w) \in \mathbb{R}^2\}$$

and for B:

$$W^s_{loc}(B) = \{(u, 0, 0) \mid u \in \mathbb{R}\} \quad W^u_{loc}(B) = \{(0, v, w) \mid (v, w) \in \mathbb{R}^2\}$$

The linearized vector field about A is

$$\begin{aligned} \dot{u} &= \lambda_A u \\ \dot{v} &= -\nu_A v \\ \dot{w} &= -\mu_A w \end{aligned}$$

and about B:

$$\begin{aligned} \dot{u} &= -\lambda_B u \\ \dot{v} &= \nu_B v \\ \dot{w} &= \mu_B w \end{aligned}$$

We now define rectangular cross sections in neighborhoods of e, $e = A, B$(see figure 15):

$$\begin{aligned} \mathcal{R}_e &= \{(u, v, w) \mid u = 1, \quad -v_e \le v \le v_e, \quad -w_e \le w \le w_e\} \\ \mathcal{R}^\mu_e &= \{(u, v, w) \mid w = 1, \quad -u_e \le u \le u_e, \quad -v_e \le v \le v_e\} \\ \mathcal{R}^\nu_e &= \{(u, v, w) \mid v = 1, \quad -u_e \le u \le u_e, \quad -w_e \le w \le w_e\} \end{aligned}$$

We can then build two first return maps $\Psi^\mu : \mathcal{R}^\mu_A \to \mathcal{R}^\mu_A$ and $\Psi^\nu : \mathcal{R}^\nu_A \to \mathcal{R}^\nu_A$ as follows: $\Psi^\mu = \Psi^\mu_{BA} \circ \Phi^\mu_B \circ \Psi_{AB} \circ \Phi^\mu_A$ and $\Psi^\nu = \Psi^\nu_{BA} \circ \Phi^\nu_B \circ \Psi_{AB} \circ \Phi^\nu_A$ where

$$\Phi^\mu_A : \mathcal{R}^\mu_A \to \mathcal{R}_A \quad \Phi^\mu_B : \mathcal{R}_B \to \mathcal{R}^\mu_B \quad \Phi^\nu_A : \mathcal{R}^\nu_A \to \mathcal{R}_A \quad \Phi^\nu_B : \mathcal{R}_B \to \mathcal{R}^\nu_B$$

$$\Psi_{AB} : \mathcal{R}_A \to \mathcal{R}_B \quad \Psi^\mu_{BA} : \mathcal{R}^\mu_B \to \mathcal{R}^\mu_A \quad \Psi^\nu_{BA} : \mathcal{R}^\nu_B \to \mathcal{R}^\nu_A$$

The local maps Φ^μ_A and Φ^ν_A are obtained by integrating the equations for the flow linearized about A:

$$\Phi^\mu_A(u, v, 1) = (1, vu^{\frac{\nu_A}{\lambda_A}}, u^{\frac{\mu_A}{\lambda_A}}) \text{ with } u \neq 0$$

$$\Phi^\nu_A(u, 1, w) = (1, u^{\frac{\nu_A}{\lambda_A}}, wu^{\frac{\mu_A}{\lambda_A}}) \text{ with } u \neq 0$$

Same thing for the maps Φ_B^μ and Φ_B^ν:

$$\Phi_B^\mu(1,v,w) = (w^{\frac{\lambda_B}{\mu_B}}, vw^{-\frac{\nu_B}{\mu_B}}, 1) \text{ with } w^{\frac{\nu_B}{\mu_B}} > v \geq 0$$

$$\Phi_B^\nu(1,v,w) = (v^{\frac{\lambda_B}{\nu_B}}, 1, wv^{-\frac{\mu_B}{\nu_B}}) \text{ with } v > w^{\frac{\nu_B}{\mu_B}} \geq 0$$

where $\mathcal{C}_B^\mu = \{(v,w) \in \mathcal{R}_B \mid w^{\frac{\nu_B}{\mu_B}} > v \geq 0\}$ and $\mathcal{C}_B^\nu = \{(v,w) \in \mathcal{R}_B \mid v > w^{\frac{\nu_B}{\mu_B}} \geq 0\}$ are complementary domains in $\mathcal{R}_B$ of the maps Φ_B^μ and Φ_B^ν. Note that the point at which a trajectory intersects $\mathcal{R}_B$ determines whether the trajectory leaves the vacinity of B in the direction of A through $\mathcal{R}_B^\mu$ or $\mathcal{R}_B^\nu$. Condition (15) implies that $\mathcal{C}_B^\mu$ is a cuspoidal region of $\mathcal{R}_B^\mu$.

By exploiting the equivariance of the vector field, we obtain for the "global" maps Ψ_{AB}, Ψ_{BA}^μ : and Ψ_{BA}^ν:

$$\Psi_{AB}(1,v,w) = (1, \alpha_{AB}v, \beta_{AB}w) + \text{h.o.t}$$
$$\Psi_{BA}^\mu(u,v,1) = (\alpha_{BA}^\mu u, \beta_{BA}^\mu v, 1) + \text{h.o.t}$$
$$\Psi_{BA}^\nu(u,1,w) = (\alpha_{BA}^\nu u, 1, \beta_{BA}^\nu w) + \text{h.o.t}$$

where the α's and β's are real coefficients.

- Study of the μ-cycle. We consider trajectories that pass through $\mathcal{R}_A^\mu$ and then travelonce through a tubular neighborhood of the μ-cycle before returning to $\mathcal{R}_A^\mu$. The behaviour of these trajectories is modelled by the return map Ψ^μ and we find to leading order:

  $$\Psi^\mu(u,v,1) = (c_1 u^{\rho_\mu}, c_2 v u^{-\sigma_\mu}, 1) \text{ with } 0 \leq v < c_3 u^{\sigma_\mu}$$

  The domain of the return map is then defined as $\mathcal{D}_A^\mu = \{(u,v) \in \mathcal{R}_A^\mu \mid 0 \leq v < c_3 u^{\sigma_\mu}\}$. A sufficient condition for $\mathcal{D}_A^\mu$ to be mapped into itself is $\sigma_\mu < 0$. This follows from the observation that the image under Ψ^μ of the bounding surface defined by the equation $v = c_3 u^{\sigma_\mu}$ is the boundary defined by $U = c_4$, where $c_4 > 0$ is some constant. Finally, if $\rho_\mu > 1$ and $\sigma_\mu < 0$ then Ψ^μ is a contraction on $\mathcal{D}_A^\mu$.

- Study of the ν-cycle. We consider trajectories that pass through $\mathcal{R}_A^\nu$ and then travelonce through a tubular neighborhood of the ν-cycle before returning to $\mathcal{R}_A^\nu$. The behaviour of these trajectories is modelled by the return map Ψ^ν and we find to leading order:

  $$\Psi^\nu(u,1,w) = (c_4 u^{\rho_\nu}, 1, c_5 w u^{-\sigma_\nu}, 1) \text{ with } 0 \leq w < c_6 u^{\sigma_\nu}$$

  The study is analogous to that for the μ-cycle. If $\rho_\nu > 1$ and $\sigma_\nu < 0$ then the ν-cycle attracts all trajectories that cross $\mathcal{R}_A^\nu$ sufficiently close to the origin.

The main difference between the results obtained for the μ-cycle and the ν-cycle comes from the condition (15). If $\rho_\nu > 1$ and $\sigma_\nu < 0$ the ν-cycle attracts almost all trajectories that lie near the heteroclinic connection from A to B, while, if $\rho_\mu > 1$ and $\sigma_\mu < 0$ the μ-cycle attracts just trajectories in a cuspoidal region emananting from the heteroclinic connection.

It is not possible that both σ_μ and σ_ν be simultaneously positive:

$$\sigma_\mu = -\frac{\nu_B}{\mu_B}\sigma_\nu$$

Note that if $\sigma_\mu > 0$ when $\rho_\nu, \rho_\mu > 1$, then almost all trajectories near the μ-cycle eventually leave it in the direction of the ν-cycle. However, since $\sigma_\nu < 0$ in this case, the trajectories that switch to the ν-cycle can not at a later time switch back to the μ-cycle.

□

5.4 Computation of the stability conditions

In principle the stability conditions stated in Theorem 6 are easy to compute. In our case however there is a difficulty which comes from the fact that for the system (14), which is truncated at order 5, the expanding and contracting eigenvalues along a given connection have exactly the same magnitude (see Table 13). It is interesting to observe that this follows from a property of reversibility of the vector field on the invariant sphere, as the next lemma shows (proof of the lemma is straightforward).

Lemma 12. *Let* $\mathbf{s}$ *be the transformation in* $\mathbb{R}^4$ *defined by* $\mathbf{s}(z_1, \bar{z}_1, z_2, \bar{z}_2) = (z_2, \bar{z}_2, z_1, \bar{z}_1)$. *Let us rewrite* $X = (z_1, \bar{z}_1, z_2, \bar{z}_2)$ *and Equation* (14) *in the form*

$$\dot{X} = (\lambda - \|X\|^2 + b\|X\|^4)X + E_{c,d}(X) \text{ with } E_{c,d}(X) = cE_{5,3}(X) + dE_{5,4}(X) \tag{16}$$

Then $E_{c,d}(\mathbf{s}X) = -\mathbf{s}E_{c,d}(X)$ *for all* X. *Moreover,* $Fix(\widetilde{C}'_{2\kappa}) = \mathbf{s}Fix(\widetilde{C}_{2\kappa})$.

Remark 5. *We recall that* $E_{5,3}$ *(resp.* $E_{5,4}$*) is the quintic equivariant map in factor of* c *(resp.* d*) in Equations* (12) *and* (13) *of Theorem 4, see Appendix C.2 for the computations.*

Now let's let $X = rU$, $U \in S^3$. The system (14) decouples in a radial part and tangential part:

$$\dot{r} = (\lambda - r^2 + br^4)r + r^5\langle E_{c,d}(U), U\rangle \tag{17}$$
$$\dot{U} = r^4[E_{c,d}(U) - \langle E_{c,d}(U), U\rangle U] = r^4 H(U) \tag{18}$$

By lemma 12 the tangential part is a reversible vector field. Let $X_0 = r_0U_0$ be an equilibrium on $\mathrm{Fix}(\widetilde{C}_{2\kappa})$ and $X'_0 = \mathbf{s}X_0 = r_0\mathbf{s}U_0$. Then X'_0 is also an equilibrium, moreover $DH(\mathbf{s}U_0) = -\mathbf{s}DH(U_0)\mathbf{s}$, which implies that the transverse eigenvalues at X'_0 are exactly opposite to the tranverse eigenvalues at X_0. This property is conserved by projection of the system on the orbit space $S^3/\mathcal{G}_0$.

It is therefore necessary to consider the 7th order expansion of the system in order to remove this degeneracy. There are 12 equivariant terms of order 7 (see Appendix B). We have checked that some of these terms are not reversible, for example the following vector field which we note E_7:

$$\begin{aligned} \dot{z}_1 &= \bar{z}_1^7 + 7\bar{z}_1^3\bar{z}_2^4 \\ \dot{z}_2 &= \bar{z}_2^7 + 7\bar{z}_2^3\bar{z}_1^4 \end{aligned}$$

Numerical simulations have been carried out with Matlab by introducing the term E_7 in the system:

$$\dot{X} = (\lambda - \|X\|^2 + b\|X\|^4)X + E_{c,d}(X) + eE_7(X) \tag{19}$$

We give in Table 14, to leading order, the transverse eigenvalues of bifurcated branches in $\mathbb{R}^4$ depending upon the parameter e of equation 19. These transverse eigenvalues allow us to compute the stability conditions of Theorem 6. For the numerical simulations, the coefficient values are $\lambda = 0.1$, $a = 0$, $b = 0.6$, $c = 1.2$ $d = 0.55$. We set $e = -1$ and we obtain:

$$\lambda_A = 0.0011 \quad \nu_A = 0.0745 \quad \mu_A = 0.0266$$

$$\lambda_B = 0.0023 \quad \nu_B = 0.0585 \quad \mu_B = 0.0215$$

which implies that:

$$\rho_\mu = 2.6336 > 1 \quad \sigma_\mu = -1.8221 < 0 \quad \rho_\nu = 2.7060 > 1 \quad \sigma_\nu = 0.6686 > 0$$

Then we are in the second case of Theorem 6. Figure 16 shows one hour runs with an initial condition close to an equilibrium with isotropy $\widetilde{C}_{2\kappa}$. For the value $e = -1$ the solution converges to a heteroclinic cycle of type μ-cycle, while for $e = 3$ none of the heteroclinic cycles are stable.

6 Conclusion

In this paper we have completed the bifurcation analysis of periodic patterns, introduced in [15], for neural field equations describing the state of a system defined on the Poincaré disk $\mathcal{D}$ when these equations are

Isotropy type	$\widetilde{C}_{2\kappa}$	$\widetilde{C}'_{2\kappa}$
$t_1(e)$	$128(3+2\sqrt{2})(b-d+(2+\sqrt{2})ex^2)x^4$	$-128(3+2\sqrt{2})(b-d-(2+\sqrt{2})ex^2)x^4$
$t_2(e)$	$-32(3+2\sqrt{2})(b+c+9d+24(2+\sqrt{2})ex^2)x^4$	$32(3+2\sqrt{2})(b+c+9d-24(2+\sqrt{2})ex^2)x^4$
$t_3(e)$	$32(3+2\sqrt{2})(b+d-3c-10(2+\sqrt{2})ex^2)x^4$	$-32(3+2\sqrt{2})(b+d-3c+10(2+\sqrt{2})ex^2)x^4$

Table 14: Transverse eigenvalues (leading order) of bifurcated branches in $\mathbb{R}^4$ depending upon the parameter e of Equation 19.

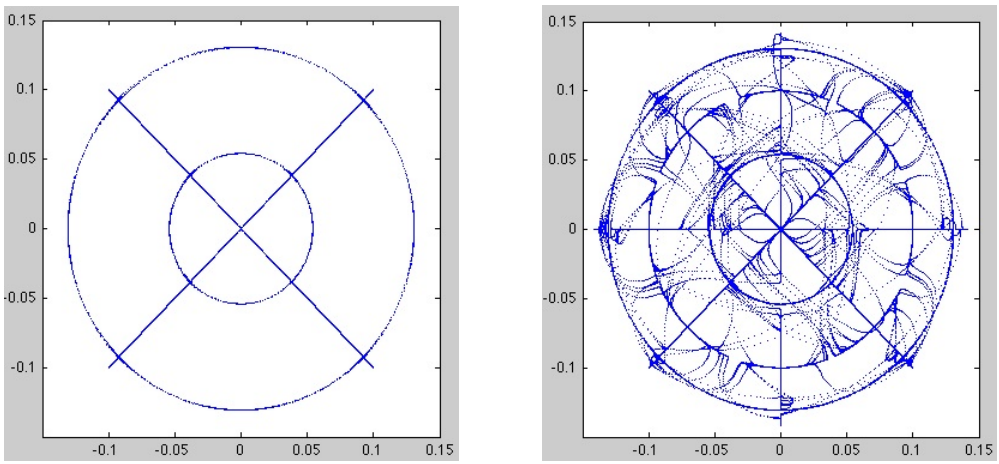

(a) $e = -1$. (b) $e = 3$.

Figure 16: Projection on the plane (x_1, y_1) of a trajectory of (19) with initial condition near an equilibrium of type $\widetilde{C}_{2\kappa}$. Coefficient values in both cases are $\lambda = 0.1$, $a = 0$, $b = 0.6$, $c = 1.2$ $d = 0.55$.

further assumed invariant under the action of the lattice group Γ of $\mathrm{U}(1,1)$ whose fundamental domain is the regular octagon. We have computed the bifurcation diagrams for the three irreducible representations of dimension four, henceforth completing the classification started in [15] (bifurcation diagrams for the representations of dimension less than four have been obtained in [15] and correspond to already well known goup actions). For two of the four-dimensional irreducible representations, we have proved that, generically, there always exist stable equilibria with a given isotropy type. For the third representation we have presented bifurcation diagrams in fixed-point planes and also shown that: (i) bifurcation of submaximal solutions can be generic, (ii) bifurcation of a heteroclinic network connecting the equilibria with maximal isotropy type can also occur generically. In the last section, we have presented a stability analysis of this heteroclinic network.

The existence of the heteroclinic network raises many interesting questions from the neuroscience point of view. Metastability in neuronal network has been observed in the brains of anaesthetized animals where the cortex seems to show intrinsic pattern of activity that evolve over time by switching among a specific set of states [30, 39, 21]. It has also been shown that metastable states play a key role in the execution of cognitive functions. Indeed, experimental and modeling studies suggest that most of these functions are the result of transient activity of large-scale brain networks in the presence of noise [37, 38]. In our case, the heteroclinic behavior of our system could be interpreted as an ongoing spontaneous activity in one hypercolumn of texture in the absence of sensory stimulus ($I_{\text{ext}} = 0$ in Equation (2)) which wanders among multiple states: each state encodes a single or several stimulus features. Our predictions should be tested experimentally. Another exciting question comes from the direct spatialization of our model. The primary visual cortex can be partitioned into fundamental domains or hypercolumns of a lattice describing the distribution of singularities or pinwheels in the orientation preference map. Bressloff and Cowan have introduced several models which take account of this functional architecture of the cortex. Their approach has led to an elegant interpretation for the occurence geometric hallucinations [10]. In our case, it would be interesting to see what kind of spatio-temporal patterns the heteroclinic behavior seen at the level of one hypercolumn could lead to in

the spatialized model. This will be the subject of future work.

Acknowledgments
The authors would like to thank R. Lauterbach for providing a GAP program to determine the action of χ_{11} and χ_{12}. This work was partially funded by the ERC advanced grant NerVi number 227747.

APPENDIX

A Presentation with biquaternions

It is natural to identify the finite group $\mathcal{G}$ to a group of 4×4 real matrices as $\dim(\chi_{12}) = 4$. Lauterbach and Matthews [36] have successfuly introduced biquaternions to study equivariant dynamical systems with $\mathbf{SO}(4)$ symmetry. Here we also use biquaterions to give a geometric way to describe the group $\mathcal{G}$. We denote by $\mathcal{Q}$ the set of unit quaternions. The set of pairs of such quaternions forms a group, called the spinor group and denoted by Spin_4. We get a map [17]:

$$\mathrm{Spin}_4 \to \mathbf{SO}(4) : (l, r) \mapsto [l, r] = \{x \mapsto \bar{l}xr\}$$

where a vector $\mathbf{x} \in \mathbb{R}^4$ is identified with a quaternion $x \in \mathbb{H}$ via

$$\mathbf{x} = \begin{pmatrix} x_1 \\ x_2 \\ x_3 \\ x_4 \end{pmatrix} \Leftrightarrow x = ex_1 + ix_2 + jx_3 + kx_4$$

The two following propositions hold.

Proposition 2. *For the irreductible representations χ_{12}, χ_{13}, the group $\mathcal{G}$ admits the following presentation with biquaternions:*

$$\mathcal{G} = \langle [j, e], \left[\frac{\sqrt{2}}{2}(j + k), j\right], [e, i], [i, e], \left[\frac{1}{2}(-e + i + j + k), \frac{1}{2}(\sqrt{3}e + i)\right] \rangle$$

It is also possible to identify the generators of $\mathcal{G}$ in matrix form:

$$\kappa = \begin{bmatrix} 0 & 0 & 0 & -1 \\ 0 & 0 & -1 & 0 \\ 0 & -1 & 0 & 0 \\ -1 & 0 & 0 & 0 \end{bmatrix}, \quad \rho = \frac{\sqrt{2}}{2}\begin{bmatrix} 0 & 0 & -1 & -1 \\ 0 & 0 & 1 & -1 \\ -1 & -1 & 0 & 0 \\ 1 & -1 & 0 & 0 \end{bmatrix}, \quad \sigma = \frac{\sqrt{2}}{4}\begin{bmatrix} 1 & \sqrt{3} & -1 & \sqrt{3} \\ \sqrt{3} & -1 & -\sqrt{3} & -1 \\ -1 & -\sqrt{3} & -1 & \sqrt{3} \\ \sqrt{3} & -1 & \sqrt{3} & 1 \end{bmatrix} \tag{20}$$

Proof. The computer algebra program GAP gives the presentation of $\mathcal{G}$ as $\mathcal{G} = \langle m_1, m_2, m_3, m_4, m_5 \rangle$ with:

$$m_1 = [j, e], m_2 = \left[\frac{\sqrt{2}}{2}(j + k), j\right], m_3 = [e, i], m_4 = [i, e], m_5 = \left[\frac{1}{2}(-e + i + j + k), \frac{1}{2}(\sqrt{3}e + i)\right]$$

We express each endomorphisms $(m_l)_{l=1\ldots5}$ of $\mathcal{G}$ in the canonical basis $\mathcal{B} = (e, i, j, k)$ and form the corresponding matrices $M_l = \mathcal{M}at_{\mathcal{B},\mathcal{B}}(m_l)$ for $l = 1 \ldots 5$. A direct calculus shows that $\mathrm{trace}(M_5) = -\sqrt{3}$ and M_5 is of order 12, such that we can write with our notations that (up to a conjugate) $M_5 = -\epsilon\kappa$. Matrices M_1, M_3, M_4 are of order 4 and M_2 of order 2. We set $\kappa = -M_1M_3$, such that $\epsilon = M_5M_1M_3$. We recognize that $M_2 = \kappa' = \rho\kappa$ then $\rho = -M_2M_1M_3$ and we verify that ρ is of order 8. A straightforward calculus shows that $\rho^2 = -M_4$ and we finally note $\sigma = \rho^{-1}\epsilon^{-1}$. The expression of the matrices of generators of $\mathcal{G}$ are given in Eq. (20). □

Proposition 3. *For the irreductible representation χ_{11}, the group $\mathcal{G}$ admits the following presentation with biquaternions:*

$$\mathcal{G} = \langle \left[\frac{1}{2}(-e + i + j + k), e\right], [e, j], [e, -e], [i, e], \left[\frac{\sqrt{2}}{2}(j + k), i\right] \rangle$$

It is also possible to identify the generators of $\mathcal{G}$ in matrix form:

$$\kappa = \begin{bmatrix} 0 & 0 & 0 & -1 \\ 0 & 0 & 1 & 0 \\ 0 & 1 & 0 & 0 \\ -1 & 0 & 0 & 0 \end{bmatrix}, \quad \rho = \frac{\sqrt{2}}{2}\begin{bmatrix} 0 & 1 & 1 & 0 \\ -1 & 0 & 0 & -1 \\ 1 & 0 & 0 & -1 \\ 0 & -1 & 1 & 0 \end{bmatrix}, \quad \sigma = \frac{\sqrt{2}}{2}\begin{bmatrix} 0 & 0 & -1 & 1 \\ 0 & 0 & 1 & 1 \\ -1 & 1 & 0 & 0 \\ 1 & 1 & 0 & 0 \end{bmatrix} \tag{21}$$

Proof. The proof is exactely the same as the previous one. □

B Molien series

In [12] we find theorems which allow to compute the vector space dimensions of the space of equivariant and invariant polynomial maps for a group action of a given degree. We recall that the set of $\mathcal{G}$-equivariant polynomial maps forms a module $\mathcal{M}$ over the ring $\mathcal{R}_\mathcal{G}$ of $\mathcal{G}$-invariant polynomial maps. We denote by $r_d = \dim \overrightarrow{\mathcal{P}}^d(\mathcal{G})$ the dimension of the polynomial equivariants of degree d.

Theorem 7 (Equivariant Molien's theorem)**.** *Consider the formal power series*

$$\Phi^\rho_\mathcal{M}(z) = \sum_{d=0}^{\infty} r_d z^d$$

It has a representation

$$\Phi^\rho_\mathcal{M}(z) = \int_\mathcal{G} \frac{Tr(g)}{\det(\mathbf{1} - z\rho(g))} dg$$

In our case, $\mathcal{G}$ is a finite group, and we can directly apply this theorem together with table 3 to find:

- for χ_{12}:

$$\Phi^{\chi_{12}}_\mathcal{M}(z) = \frac{1}{96}\left[\frac{4}{(1-z)^4} - \frac{4}{(1+z)^4} + \frac{8}{1-z-z^3+z^4} - \frac{8}{1+z+z^3+z^4} + \frac{8\sqrt{3}}{1-z\sqrt{3}+2z^2-z^3\sqrt{3}+z^4} - \frac{8\sqrt{3}}{1+z\sqrt{3}+2z^2+z^3\sqrt{3}+z^4}\right]$$

  and $\Phi^{\chi_{12}}_\mathcal{M}(z) = z + 2z^3 + 5z^5 + 10z^7 + O(z^7)$.

- for χ_{11}:

$$\Phi^{\chi_{11}}_\mathcal{M}(z) = \frac{1}{96}\left[\frac{4}{(1-z)^4} - \frac{4}{(1+z)^4} - \frac{16}{(1+z+z^2)^2} + \frac{16}{(1-z+z^2)^2}\right]$$

  and $\Phi^{\chi_{11}}_\mathcal{M}(z) = z + z^3 + 4z^5 + 12z^7 + O(z^7)$.

An analog of the Equivariant Molien's theorem holds for invariant polynomial mapsa dn we denote $c_d = \dim \mathcal{R}^d$ the dimension of invariants polynomials of degree d.

Theorem 8 (Invariant Molien's theorem)**.** *Consider the formal power series*

$$P^\rho_{\mathcal{R}_\mathcal{G}}(z) = \sum_{d=0}^{\infty} c_d z^d$$

It has a representation

$$P^\rho_{\mathcal{R}_\mathcal{G}}(z) = \int_\mathcal{G} \frac{1}{\det(\mathbf{1} - z\rho(g))} dg$$

Applying this theorem together with tables 1 and 2 yields

- for χ_{12}:

$$P^{\chi_{12}}_{\mathcal{R}_\mathcal{G}}(z) = z^2 + 2z^4 + 3z^6 + O(z^6)$$

- for χ_{11}:

$$P^{\chi_{11}}_{\mathcal{R}_\mathcal{G}}(z) = z^2 + z^4 + 3z^6 + O(z^6)$$

These results are summerized in the following table:

Character	e3	i4	e5	i6	e7
χ_{11}	1	1	4	3	12
χ_{12}	2	2	5	3	10
χ_{13}	2	2	5	3	10

Table 15: The information on the number of invariant/equivariant polynomial maps for the irreductible representations χ_{11}, χ_{12} and χ_{13}. Here e stands for equivariant, i for invariant and the number behind these letters for the degree of the polynomial map. The number in the table gives the dimension of the space of equivariant/invariant polynomial maps in the given degrees.

C Computation of low-order equivariants

C.1 Computational part of the proof of theorem 2

Proposition 4. *For the irreductible representation χ_{12}, the two cubic equivariant maps are:*

$$E_1(\mathbf{z}) = \mathbf{z}\left(|z_1|^2 + |z_2|^2\right) \text{ and } E_2(\mathbf{z}) = \begin{bmatrix} \sqrt{3}\left(3z_1^2 + \bar{z}_2^2\right)\bar{z}_1 - \mathbf{i}\left(z_2^2 + 3\bar{z}_1^2\right)z_2 \\ \sqrt{3}\left(3\bar{z}_1^2 + z_2^2\right)z_1 + \mathbf{i}\left(\bar{z}_2^2 + 3z_1^2\right)\bar{z}_2 \\ \sqrt{3}\left(3z_2^2 + \bar{z}_1^2\right)\bar{z}_2 + \mathbf{i}\left(z_1^2 + 3\bar{z}_2^2\right)z_1 \\ \sqrt{3}\left(3\bar{z}_2^2 + z_1^2\right)z_2 - \mathbf{i}\left(\bar{z}_1^2 + 3z_2^2\right)\bar{z}_1 \end{bmatrix} \tag{22}$$

Proof. Let E denote a homogeneous equivariant mapping. We want to deduce the restrictions placed on the form of E by the symmetry group $\mathcal{G}$. We first choose appropriate coordinates. Thanks to proposition 2 of appendix A we have a presentation of $\mathcal{G}$ with 4×4 real matrices with generators ρ, σ, κ given by equation Eq 20. The eigenvalues of ρ are $\exp(\pm\frac{\mathbf{i}\pi}{4}), \exp(\pm\frac{3\mathbf{i}\pi}{4})$ (where $\mathbf{i}^2 = -1$). And we have the following decomposition:

$$\rho_P = P^{-1}\rho P = \begin{bmatrix} \exp(\frac{\mathbf{i}\pi}{4}) & 0 & 0 & 0 \\ 0 & \exp(-\frac{\mathbf{i}\pi}{4}) & 0 & 0 \\ 0 & 0 & \exp(\frac{3\mathbf{i}\pi}{4}) & 0 \\ 0 & 0 & 0 & \exp(-\frac{3\mathbf{i}\pi}{4}) \end{bmatrix} \text{ with } P = \begin{bmatrix} \mathbf{i} & -\mathbf{i} & \mathbf{i} & -\mathbf{i} \\ -1 & -1 & 1 & 1 \\ -\mathbf{i} & \mathbf{i} & \mathbf{i} & -\mathbf{i} \\ 1 & 1 & 1 & 1 \end{bmatrix}$$

Then we can express in this basis the other generators:

$$\sigma_P = P^{-1}\sigma P = \frac{\sqrt{2}}{4}\begin{bmatrix} 1 & \mathbf{i}\sqrt{3} & 1 & -\mathbf{i}\sqrt{3} \\ -\mathbf{i}\sqrt{3} & 1 & \mathbf{i}\sqrt{3} & 1 \\ 1 & -\mathbf{i}\sqrt{3} & -1 & -\mathbf{i}\sqrt{3} \\ \mathbf{i}\sqrt{3} & 1 & \mathbf{i}\sqrt{3} & -1 \end{bmatrix} \text{ and } \kappa_P = P^{-1}\kappa P = \begin{bmatrix} 0 & \mathbf{i} & 0 & 0 \\ -\mathbf{i} & 0 & 0 & 0 \\ 0 & 0 & 0 & \mathbf{i} \\ 0 & 0 & -\mathbf{i} & 0 \end{bmatrix}$$

We denote $\mathbf{z} = (z_1, \bar{z}_1, z_2, \bar{z}_2)$ the complex coordinates associated to the eigenvectors of ρ i.e the columns of P. Write E in components as $(f_1, \bar{f}_1, f_2, \bar{f}_2)^{\mathbf{T}}$. We begin by describing the action of ρ_P on the equivariant map E.

For all $\mathbf{z}$, the action is given by $\rho_P \cdot \mathbf{z} = (e^{\frac{\mathbf{i}\pi}{4}}z_1, e^{-\frac{\mathbf{i}\pi}{4}}\bar{z}_1, e^{\frac{3\mathbf{i}\pi}{4}}z_2, e^{-\frac{3\mathbf{i}\pi}{4}}\bar{z}_2)$ and the equivariance yields

$$\begin{cases} e^{\frac{\mathbf{i}\pi}{4}}f_1(z_1, \bar{z}_1, z_2, \bar{z}_2) = f_1(e^{\frac{\mathbf{i}\pi}{4}}z_1, e^{-\frac{\mathbf{i}\pi}{4}}\bar{z}_1, e^{\frac{3\mathbf{i}\pi}{4}}z_2, e^{-\frac{3\mathbf{i}\pi}{4}}\bar{z}_2) \\ e^{\frac{\mathbf{i}3\pi}{4}}f_2(z_1, \bar{z}_1, z_2, \bar{z}_2) = f_2(e^{\frac{\mathbf{i}\pi}{4}}z_1, e^{-\frac{\mathbf{i}\pi}{4}}\bar{z}_1, e^{\frac{3\mathbf{i}\pi}{4}}z_2, e^{-\frac{3\mathbf{i}\pi}{4}}\bar{z}_2) \end{cases} \tag{23}$$

We are looking for cubic equivariants of the form $\alpha z_1^{k_1}\bar{z}_1^{l_1}z_2^{k_2}\bar{z}_2^{l_2}$ satisfying the relation $k_1+k_2+l_1+l_2 = 3$. So with the first equation of (23) we simply get

$$\alpha e^{\frac{\mathbf{i}\pi}{4}}z_1^{k_1}\bar{z}_1^{l_1}z_2^{k_2}\bar{z}_2^{l_2} = \alpha e^{\mathbf{i}\frac{\pi}{4}[(k_1-l_1)+3(k_2-l_2)]}z_1^{k_1}\bar{z}_1^{l_1}z_2^{k_2}\bar{z}_2^{l_2}$$

In order that this is equivariant under the action of ρ_P we have to impose:

$$(k_1 - l_1 - 1) + 3(k_2 - l_2) = 8n \text{ with } n \in \mathbb{Z}$$

which gives 5 elements in f_1.

$$f_1(z_1,\bar{z}_1,z_2,\bar{z}_2) = a_1 z_1^2\bar{z}_1 + a_2 z_1 z_2\bar{z}_2 + a_3 z_2^3 + a_4\bar{z}_1^2 z_2 + a_5\bar{z}_1\bar{z}_2^2$$

with $(a_i)_{i=1\dots5} \in \mathbb{C}^5$. In the same fashion the second equation of (23) gives 5 elements in f_2.

$$f_2(z_1,\bar{z}_1,z_2,\bar{z}_2) = b_1 z_2^2\bar{z}_2 + b_2 z_1\bar{z}_1 z_2 + b_3 z_1^3 + b_4 z_1\bar{z}_2^2 + b_5\bar{z}_1^2\bar{z}_2$$

with $(b_i)_{i=1\dots5} \in \mathbb{C}^5$.

The action of κ_P on $\mathbf{z}$ is given by $\kappa_P \cdot \mathbf{z} = (\mathbf{i}\bar{z}_1, -\mathbf{i}z_1, \mathbf{i}\bar{z}_2, -\mathbf{i}z_2)$. It is straightforward to see that this action imposes that $a_1, a_2, a_5, b_1, b_2, b_5$ are real and that a_3, a_4, b_3, b_4 are imaginary numbers. Then we can rewrite f_1 and f_2 as:

$$f_1(z_1,\bar{z}_1,z_2,\bar{z}_2) = \alpha_1 z_1^2\bar{z}_1 + \alpha_2 z_1 z_2\bar{z}_2 + \mathbf{i}\alpha_3 z_2^3 + \mathbf{i}\alpha_4\bar{z}_1^2 z_2 + \alpha_5\bar{z}_1\bar{z}_2^2$$

$$f_2(z_1,\bar{z}_1,z_2,\bar{z}_2) = \beta_1 z_2^2\bar{z}_2 + \beta_2 z_1\bar{z}_1 z_2 + \mathbf{i}\beta_3 z_1^3 + \mathbf{i}\beta_4 z_1\bar{z}_2^2 + \beta_5\bar{z}_1^2\bar{z}_2$$

with $(\alpha_i, \beta_i)_{i=1\dots5} \in (\mathbb{R}\times\mathbb{R})^5$.

Action of σ_P:

The action of σ_P on $\mathbf{z}$ is given by

$$\sigma_P \cdot \mathbf{z} = \begin{pmatrix} \frac{\sqrt{2}}{4}\left(z_1 + z_2 + \mathbf{i}\sqrt{3}(\bar{z}_1 - \bar{z}_2)\right) \\ \frac{\sqrt{2}}{4}\left(\bar{z}_1 + \bar{z}_2 - \mathbf{i}\sqrt{3}(z_1 - z_2)\right) \\ \frac{\sqrt{2}}{4}\left(z_1 - z_2 - \mathbf{i}\sqrt{3}(\bar{z}_1 + \bar{z}_2)\right) \\ \frac{\sqrt{2}}{4}\left(\bar{z}_1 - \bar{z}_2 + \mathbf{i}\sqrt{3}(z_1 + z_2)\right) \end{pmatrix}^{\mathbf{T}}$$

and we find:

$$f_1(z_1,\bar{z}_1,z_2,\bar{z}_2) = a z_1(|z_1|^2 + |z_2|^2) + b\left(3\sqrt{3}z_1|z_1|^2 - \mathbf{i}z_2^3 - 3\mathbf{i}\bar{z}_1^2 z_2 + \sqrt{3}\bar{z}_1\bar{z}_2^2\right)$$

$$f_2(z_1,\bar{z}_1,z_2,\bar{z}_2) = a z_2(|z_1|^2 + |z_2|^2) + b\left(3\sqrt{3}z_2|z_2|^2 + \mathbf{i}z_1^3 + 3\mathbf{i}z_1\bar{z}_2^2 + \sqrt{3}\bar{z}_1^2\bar{z}_2\right)$$

with $(a,b) \in \mathbb{R}^2$.

□

C.2 Computational part of the proof of theorem 4

Proposition 5. *For the irreductible representation χ_{11}, the four quintic equivariant maps are:*

$$E_{5,1}(\mathbf{z}) = \mathbf{z}\|\mathbf{z}\|^4, \quad E_{5,2} = \begin{bmatrix} z_1^4\bar{z}_2 + 4z_2^3|z_1|^2 - z_2^3|z_2|^2 \\ \bar{z}_1^4 z_2 + 4\bar{z}_2^3|z_1|^2 - \bar{z}_2^3|z_2|^2 \\ -\bar{z}_1 z_2^4 - 4z_1^3|z_2|^2 + z_1^3|z_1|^2 \\ -z_1\bar{z}_2^4 - 4\bar{z}_1^3|z_2|^2 + \bar{z}_1^3|z_1|^2 \end{bmatrix}$$

$$E_{5,3} = \begin{bmatrix} 3\bar{z}_1^2 z_2|z_2|^2 - z_1^2\bar{z}_2^3 - 2\bar{z}_1^2|z_1|^2 z_2 \\ 3z_1^2\bar{z}_2|z_2|^2 - \bar{z}_1^2 z_2^3 - 2z_1^2|z_1|^2\bar{z}_2 \\ -3z_1\bar{z}_2^2|z_1|^2 + \bar{z}_1^3 z_2^2 + 2z_1\bar{z}_2^2|z_2|^2 \\ -3\bar{z}_1 z_2^2|z_1|^2 + z_1^3\bar{z}_2^2 + 2\bar{z}_1 z_2^2|z_2|^2 \end{bmatrix}, \quad E_{5,4} = \begin{bmatrix} -5\bar{z}_1^4\bar{z}_2 + \bar{z}_2^5 \\ -5z_1^4 z_2 + z_2^5 \\ 5\bar{z}_1\bar{z}_2^4 - \bar{z}_1^5 \\ 5z_1 z_2^4 - z_1^5 \end{bmatrix}$$

Proof. Let E denote a homageneous cubic equivariant mapping. Thanks to proposition 3 of appendix A the generators of $\mathcal{G}$ are given in matrix form in equation (21). The eigenvalues of ρ are still $\exp(\pm\frac{\mathbf{i}\pi}{4}), \exp(\pm\frac{3\mathbf{i}\pi}{4})$. And we have the following decomposition:

$$\rho_P = P^{-1}\rho P = \begin{bmatrix} \exp(\frac{\mathbf{i}\pi}{4}) & 0 & 0 & 0 \\ 0 & \exp(-\frac{\mathbf{i}\pi}{4}) & 0 & 0 \\ 0 & 0 & \exp(\frac{3\mathbf{i}\pi}{4}) & 0 \\ 0 & 0 & 0 & \exp(-\frac{3\mathbf{i}\pi}{4}) \end{bmatrix} \text{ with } P = \begin{bmatrix} \mathbf{i} & -\mathbf{i} & -\mathbf{i} & \mathbf{i} \\ -1 & -1 & 1 & 1 \\ \mathbf{i} & -\mathbf{i} & \mathbf{i} & -\mathbf{i} \\ 1 & 1 & 1 & 1 \end{bmatrix}$$

Then we can express in this basis the other generators:

$$\sigma_P = P^{-1}\sigma P = \frac{\sqrt{2}}{2}\begin{bmatrix} -1 & 0 & -\mathbf{i} & 0 \\ 0 & -1 & 0 & \mathbf{i} \\ \mathbf{i} & 0 & 1 & 0 \\ 0 & -\mathbf{i} & 0 & 1 \end{bmatrix} \text{ and } \kappa_P = P^{-1}\kappa P = \begin{bmatrix} 0 & \mathbf{i} & 0 & 0 \\ -\mathbf{i} & 0 & 0 & 0 \\ 0 & 0 & 0 & -\mathbf{i} \\ 0 & 0 & \mathbf{i} & 0 \end{bmatrix}$$

We denote $\mathbf{z} = (z_1, \bar{z}_1, z_2, \bar{z}_2)$ the complex coordinates associated to the eigenvectors of ρ i.e the columns of P. Write E in components as $(f_1, \bar{f}_1, f_2, \bar{f}_2)^{\mathbf{T}}$. The action of ρ_P on a quintic equivariant map of the form $\alpha z_1^{k_1}\bar{z}_1^{l_1}z_2^{k_2}\bar{z}_2^{l_2}$ with the relation $k_1+k_2+l_1+l_2 = 5$ implies that $(k_1-l_1-1)+3(k_2-l_2) = 8n$ with $n \in \mathbb{Z}$, which gives 14 elements in f_1.

$$f_1(z_1, \bar{z}_1, z_2, \bar{z}_2) = a_1 z_1^3\bar{z}_1^2 + a_2 z_1 z_2^2\bar{z}_2^2 + a_3 z_1^2\bar{z}_1 z_2\bar{z}_2 + a_4 z_1^4\bar{z}_2 + a_5\bar{z}_1^2 z_2^2\bar{z}_2 + a_6 z_1\bar{z}_1 z_2^3 + a_7 z_1^3 z_2^2$$
$$+a_8 z_2^4\bar{z}_2 + a_9 z_1^2\bar{z}_2^3 + a_{10} z_1\bar{z}_1^2\bar{z}_2^2 + a_{11}\bar{z}_1 z_2\bar{z}_2^3 + a_{12}\bar{z}_1^4\bar{z}_2 + a_{13}\bar{z}_2^5 + a_{14} z_1\bar{z}_1^3 z_2$$

And we also obtain 14 elements in f_2 with the same method:

$$f_2(z_1, \bar{z}_1, z_2, \bar{z}_2) = b_1 z_1^2\bar{z}_1^2 z_2 + b_2 z_1\bar{z}_1 z_2^2\bar{z}_2 + b_3 z_2^3\bar{z}_2^2 + b_4 z_1^4\bar{z}_1 + b_5 z_1^3 z_2\bar{z}_2 + b_6\bar{z}_1^3 z_2^2 + b_7 z_1^2 z_2^3$$
$$+b_8\bar{z}_1 z_2^4 + b_9 z_1 z_2\bar{z}_2^3 + b_{10} z_1^2\bar{z}_1\bar{z}_2^2 + b_{11} z_1\bar{z}_1^3\bar{z}_2 + b_{12}\bar{z}_1^2 z_2\bar{z}_2^2 + b_{13}\bar{z}_1^5 + b_{14}\bar{z}_1\bar{z}_2^4$$

where $(a_j)_{j=1\ldots14} \in \mathbb{C}^{14}$ and $(b_j)_{j=1\ldots14} \in \mathbb{C}^{14}$.

The action of κ_P implies that the coefficients $(a_j, b_j)_{j=1\ldots14}$ are real. The action of σ_P is $\sigma_P \cdot \mathbf{z} = \frac{\sqrt{2}}{2}(-z_1 - \mathbf{i}z_2, -\bar{z}_1 + \mathbf{i}\bar{z}_2, \mathbf{i}z_1 + z_2, -\mathbf{i}\bar{z}_1 + \bar{z}_2)$ and we obtain:

$$f_1(z_1, \bar{z}_1, z_2, \bar{z}_2) = a(z_1|z_1|^4 + z_1|z_2|^4 + 2z_1|z_1|^2|z_2|^2) + b(z_1^4\bar{z}_2 + 4z_2^3|z_1|^2 - z_2^3|z_2|^2)$$
$$+c(3\bar{z}_1^2 z_2|z_2|^2 - z_1^2\bar{z}_2^3 - 2\bar{z}_1^2|z_1|^2 z_2) + d(-5\bar{z}_1^4\bar{z}_2 + \bar{z}_2^5)$$
$$f_2(z_1, \bar{z}_1, z_2, \bar{z}_2) = a(z_2|z_2|^4 + z_2|z_1|^4 + 2z_2|z_1|^2|z_2|^2) + b(-\bar{z}_1 z_2^4 - 4z_1^3|z_2|^2 + z_1^3|z_1|^2)$$
$$+c(-3z_1\bar{z}_2^2|z_1|^2 + \bar{z}_1^3 z_2^2 + 2z_1\bar{z}_2^2|z_2|^2) + d(5\bar{z}_1\bar{z}_2^4 - \bar{z}_1^5)$$

with $(a, b, c, d) \in \mathbb{R}^4$. Thus, we find 4 equivariant maps which is in agreement with computation of the Molien serie of appendix B. □

D Fixed-point subspaces

D.1 Proof of Lemma 7

To complete the proof of Lemma 7 we give the matrix of $\sigma, \tilde{\sigma}, \epsilon, \kappa, \kappa'$ and κ'' in the basis associated to coordinates $(z_1, \bar{z}_1, z_2, \bar{z}_2)$.

$$\sigma = \frac{\sqrt{2}}{4}\begin{bmatrix} 1 & \mathbf{i}\sqrt{3} & 1 & -\mathbf{i}\sqrt{3} \\ -\mathbf{i}\sqrt{3} & 1 & \mathbf{i}\sqrt{3} & 1 \\ 1 & -\mathbf{i}\sqrt{3} & -1 & -\mathbf{i}\sqrt{3} \\ \mathbf{i}\sqrt{3} & 1 & \mathbf{i}\sqrt{3} & -1 \end{bmatrix}, \quad \tilde{\sigma} = \frac{\sqrt{2}}{4}\begin{bmatrix} 1 & -\mathbf{i}\sqrt{3} & -1 & -\mathbf{i}\sqrt{3} \\ \mathbf{i}\sqrt{3} & 1 & \mathbf{i}\sqrt{3} & -1 \\ -1 & -\mathbf{i}\sqrt{3} & -1 & \mathbf{i}\sqrt{3} \\ \mathbf{i}\sqrt{3} & -1 & -\mathbf{i}\sqrt{3} & -1 \end{bmatrix}$$

$$\epsilon = \frac{1}{4}\begin{bmatrix} 1-\mathbf{i} & \sqrt{3}(\mathbf{i}-1) & -1-\mathbf{i} & \sqrt{3}(1+\mathbf{i}) \\ -\sqrt{3}(1+\mathbf{i}) & 1+\mathbf{i} & \sqrt{3}(1-\mathbf{i}) & \mathbf{i}-1 \\ 1-\mathbf{i} & \sqrt{3}(1-\mathbf{i}) & 1+\mathbf{i} & \sqrt{3}(1+\mathbf{i}) \\ \sqrt{3}(1+\mathbf{i}) & 1+\mathbf{i} & \sqrt{3}(1-\mathbf{i}) & 1-\mathbf{i} \end{bmatrix}, \quad \kappa = \begin{bmatrix} 0 & \mathbf{i} & 0 & 0 \\ -\mathbf{i} & 0 & 0 & 0 \\ 0 & 0 & 0 & \mathbf{i} \\ 0 & 0 & -\mathbf{i} & 0 \end{bmatrix}$$

$$\kappa' = \frac{\sqrt{2}}{2}\begin{bmatrix} 0 & \mathbf{i}-1 & 0 & 0 \\ -1-\mathbf{i} & 0 & 0 & 0 \\ 0 & 0 & 0 & -1-\mathbf{i} \\ 0 & 0 & -1+\mathbf{i} & 0 \end{bmatrix}, \quad \kappa'' = \frac{\sqrt{2}}{4}\begin{bmatrix} \sqrt{3} & \mathbf{i} & -\sqrt{3} & \mathbf{i} \\ -\mathbf{i} & \sqrt{3} & -\mathbf{i} & -\sqrt{3} \\ -\sqrt{3} & \mathbf{i} & -\sqrt{3} & -\mathbf{i} \\ -\mathbf{i} & -\sqrt{3} & \mathbf{i} & -\sqrt{3} \end{bmatrix}$$

D.2 Proof of Lemma 10

To complete the proof of Lemma 10 we give the matrix of σ, κ, κ' and κ'' in the basis associated to coordinates $(z_1, \bar{z}_1, z_2, \bar{z}_2)$.

$$\sigma = \frac{\sqrt{2}}{2}\begin{bmatrix} -1 & 0 & -\mathbf{i} & 0 \\ 0 & -1 & 0 & \mathbf{i} \\ \mathbf{i} & 0 & 1 & 0 \\ 0 & -\mathbf{i} & 0 & 1 \end{bmatrix}, \quad \kappa = \begin{bmatrix} 0 & \mathbf{i} & 0 & 0 \\ -\mathbf{i} & 0 & 0 & 0 \\ 0 & 0 & 0 & -\mathbf{i} \\ 0 & 0 & \mathbf{i} & 0 \end{bmatrix}$$

$$\kappa' = \frac{\sqrt{2}}{2}\begin{bmatrix} 0 & \mathbf{i}-1 & 0 & 0 \\ -1-\mathbf{i} & 0 & 0 & 0 \\ 0 & 0 & 0 & 1+\mathbf{i} \\ 0 & 0 & 1-\mathbf{i} & 0 \end{bmatrix}, \quad \kappa'' = \frac{\sqrt{2}}{2}\begin{bmatrix} 0 & -\mathbf{i} & 0 & -1 \\ \mathbf{i} & 0 & -1 & 0 \\ 0 & -1 & 0 & -\mathbf{i} \\ -1 & 0 & \mathbf{i} & 0 \end{bmatrix}$$

References

[1] M.A.D. Aguiar, S.B.S.D. Castro, and I.S. Labouriau. Dynamics near a heteroclinic network. *Nonlinearity*, 18, 2005.

[2] D. Armbruster, J. Guckenheimer and P. Holmes Heteroclinic cycles and modulated waves in systems with O(2) symmetry. *Phyisica D*, 29, 257–282, 1988.

[3] P. Ashwin and M. Field. Heteroclinic networks in coupled cell systems. *Archive for Rational Mechanics and Analysis*, 148(2):107–143, 1999.

[4] R. Aurich and F. Steiner. Periodic-orbit sum rules for the hadamard-gutzwiller model. *Physica D*, 39:169–193, 1989.

[5] N.L. Balazs and A. Voros. Chaos on the pseudosphere. *Physics Reports*, 143(3):109–240, 1986.

[6] J. Bigun and G. Granlund. Optimal orientation detection of linear symmetry. In *Proc. First Int'l Conf. Comput. Vision*, pages 433–438. EEE Computer Society Press, 1987.

[7] P. C. Bressloff and J. D. Cowan. A spherical model for orientation and spatial frequency tuning in a cortical hypercolumn. *Philosophical Transactions of the Royal Society B*, 2003.

[8] P.C. Bressloff and J.D. Cowan. SO(3) symmetry breaking mechanism for orientation and spatial frequency tuning in the visual cortex. *Phys. Rev. Lett.*, 88(7), feb 2002.

[9] P.C. Bressloff and J.D. Cowan. The visual cortex as a crystal. *Physica D: Nonlinear Phenomena*, 173(3–4):226–258, dec 2002.

[10] P.C. Bressloff, J.D. Cowan, M. Golubitsky, P.J. Thomas, and M.C. Wiener. Geometric visual hallucinations, Euclidean symmetry and the functional architecture of striate cortex. *Phil. Trans. R. Soc. Lond. B*, 306(1407):299–330, mar 2001.

[11] P. Chossat and R. Lauterbach. Le théorème de hartman-grobman et la réduction à l'espace des orbites. *Comptes Rendus de l'Académie des Sciences-Series I-Mathematics*, 325(6):595–600, 1997.

[12] P. Chossat and R. Lauterbach. Methods in Equivariant Bifurcations and Dynamical Systems. *World Scientific Publishing Company*, 2000.

[13] P. Chossat, R. Lauterbach, and I. Melbourne. Steady-state bifurcation with 0 (3)-symmetry. *Archive for Rational Mechanics and Analysis*, 113(4):313–376, 1990.

[14] Pascal Chossat and Olivier Faugeras. Hyperbolic planforms in relation to visual edges and textures perception. *Plos Comput Biol*, 5(12):e1000625, December 2009.

[15] Pascal Chossat, Grégory Faye, and Olivier Faugeras. Bifurcation of hyperbolic planforms. *Journal of Nonlinear Science*, February 2011.

[16] P.G. Ciarlet and J.L. Lions, editors. Handbook of Numerical Analysis. Volume II. Finite Element Methods (part1). *North-Holland*, 1991.

[17] J.H Conway and D.A Smith. On Quaternions and Octonions, Their Geometry, Arithmetic, and Symmetry. *AK Peters*, 2003.

[18] A. Fässler and E.L. Stiefel. Group theoretical methods and their applications. *Birkhäuser*, 1992.

[19] M. Field. Equivariant bifurcation theory and symmetry breaking. *Journal of Dynamics and Differential Equations*, 1(4):369–421, 1989.

[20] M. Field. Lectures on bifurcations, dynamics and symmetry. *Pitman Research Notes in Mathematics Series*, 1996.

[21] J.A. Goldberg, U. Rokni and H. Sompolinsky. Patterns of ongoing activity and the functional architecture of the primary visual cortex. *Neuron, vol 42, pp 489–500, 2004.*

[22] M. Golubitsky, I. Stewart, and D.G. Schaeffer. Singularities and Groups in Bifurcation Theory, volume II. *Springer*, 1988.

[23] J. Guckenheimer and P. Holmes Structurally stable heteroclinic cycles. Math. Proc. Cambridge Phil. Soc. 103, 189–192, 1988.

[24] V. Guillemin and A. Pollack. Differential topology. *Chelsea Pub Co*, 2010.

[25] M. Haragus and G. Iooss. Local bifurcations, center manifolds, and normal forms in infinite dimensional systems. *EDP Sci. Springer Verlag UTX series*, 2010.

[26] P. Hartman. *Ordinary differential equations*, volume 38. Classics in Applied Mathematics, siam edition, 2002.

[27] S. Helgason. Groups and geometric analysis, volume 83 of *Mathematical Surveys and Monographs. American Mathematical Society*, 2000.

[28] R.B. Hoyle. Pattern formation: an introduction to methods. *Cambridge Univ Pr*, 2006.

[29] S. Katok. Fuchsian Groups. *Chicago Lectures in Mathematics. The University of Chicago Press*, 1992.

[30] T. Kenet, D. Bibitchkov, M. Tsodyks, A. Grinvald and A. Arieli. Spontaneously emerging cortical representations of visual attributes. *Nature*, vol 425, issue 6961, pp 954–956, 2003.

[31] V. Kirk and M. Silber. A competition between heteroclinic cycles. *Nonlinearity*, 7:1605, 1994.

[32] H. Knutsson. Representing local structure using tensors. In *Scandinavian Conference on Image Analysis*, pages 244–251, 1989.

[33] M. Krupa and I. Melbourne. Nonasymptotically stable attractors in o(2) mode interactions. *Normal forms and homoclinic chaos (Waterloo, ON, 1992)*, 4:219–232, 1992.

[34] M. Krupa and I. Melbourne. Asymptotic stability of heteroclinic cycles in systems with symmetry. *Ergodic Theory and Dynamical Systems*, 15(01):121–147, 1995.

[35] M. Krupa and I. Melbourne. Asymptotic stability of heteroclinic cycles in systems with symmetry. ii. *Proceedings of the Royal Society of Edinburgh: Section A Mathematics*, 134(06):1177–1197, 2004.

[36] R. Lauterbach and P. Matthews. Do absolutely irreducible group actions have odd dimensional fixed point spaces? *ArXiv*, (1011.3986), 2010.

[37] M.I. Rabinovich, R. Huerta, P. Varona and V.S. Afraimovich. Transient cognitive dynamics, metastability, and decision making *PLoS Comput. Biol*, e1000072, 2008.

[38] M.I. Rabinovich, M.K. Muezzinoglu, I.Strigo and A. Bystritsky. Dynamical Principles of Emotion-Cognition Interaction: Mathematical Images of Mental Disorders . *PloS One*, e12547, 2010.

[39] D.L. Ringach. Neuroscience: states of mind. *Nature* , vol 425, 2003.

[40] C. Schmit. Quantum and classical properties of some billiards on the hyperbolic plane. *Chaos and Quantum Physics*, pages 335–369, 1991.

[41] H.R. Wilson and J.D. Cowan. Excitatory and inhibitory interactions in localized populations of model neurons. *Biophys. J.*, 12:1–24, 1972.

[42] H.R. Wilson and J.D. Cowan. A mathematical theory of the functional dynamics of cortical and thalamic nervous tissue. *Biological Cybernetics*, 13(2):55–80, September 1973.